



Cite this: RSC Adv., 2014, 4, 37003

## Principles and mechanisms of photocatalytic dye degradation on $\text{TiO}_2$ based photocatalysts: a comparative overview

Anila Ajmal,<sup>a</sup> Imran Majeed,<sup>b</sup> Riffat Naseem Malik,<sup>a</sup> Hicham Idriss<sup>c</sup> and Muhammad Amtiaz Nadeem<sup>\*ac</sup>

The total annual production of synthetic dye is more than  $7 \times 10^5$  tons. Annually, through only textile waste effluents, around one thousand tons of non-biodegradable textile dyes are discharged into natural streams and water bodies. Therefore, with growing environmental concerns and environmental awareness there is a need for the removal of dyes from local and industrial water effluents with a cost effective technology. In general, these dyes have been found to be resistant to biological as well as physical treatment technologies. In this regard, heterogeneous advanced oxidation processes (AOPs), involving photo-catalyzed degradation of dyes using semiconductor nanoparticles is considered as an efficient cure for dye pollution. In the last two decades  $\text{TiO}_2$  has received considerable interest because of its high potential as a photocatalyst to degrade a wide range of organic material including dyes. This review starts with (i) a brief overview on dye pollution, dye classification and dye decolourization/degradation strategies; (ii) focuses on the mechanisms involved in comparatively well understood  $\text{TiO}_2$  photocatalysts and (iii) discusses recent advancements to enhance  $\text{TiO}_2$  photocatalytic efficiency by (a) doping with metals, non-metals, transition metals, noble metals and lanthanide ions, (b) structural modifications of  $\text{TiO}_2$  and (c) immobilization of  $\text{TiO}_2$  by using various supports to make it a flexible and cost-effective commercial dye treatment technology.

Received 4th July 2014

Accepted 4th August 2014

DOI: 10.1039/c4ra06658h

[www.rsc.org/advances](http://www.rsc.org/advances)

### Dye pollution-an overview

Dyes play a vital role in various branches of the dyeing and textile industries. Over 100 000 commercially available synthetic dyes are the most frequently used dyes in such industries. These dyes are usually derived from two main sources *i.e.* coal tar and petroleum intermediates with a total annual production of more than  $7 \times 10^5$  tons.<sup>5–7</sup> Annually, through textile waste effluents, around 15% (one thousand

tons) of these non-biodegradable textile dyes are discharged into natural streams and water bodies.<sup>1–4,8,9</sup> Typically, on an average for every kilogram of cloth, being processed in dyeing and finishing plants, about 120–280 L of water is being consumed.<sup>10</sup>

Konstantinou and Albanis<sup>11</sup> reported that industrial dye stuffs and textile dyes constitute one of the largest groups of toxic organic compounds. According to an estimate made by World Bank, nearly 17–20% water pollution has the major contributors related to textile finishing and dyeing industries. According to a study by Kant, out of major identified wastewater toxic chemicals, 72 chemicals were solely released by the textile dyeing and nearly 30 of such chemicals were not treatable.<sup>12</sup> In

<sup>a</sup>Department of Environmental Sciences, Quaid-i-Azam University, Islamabad 4200, Pakistan. E-mail: NadeemMI@SABIC.com

<sup>b</sup>Department of Chemistry, Quaid-i-Azam University, Islamabad 4200, Pakistan

<sup>c</sup>CRI-KAUST, Saudi Basic Industries Corporation, Thuwal, Saudi Arabia

Anila Ajmal has recently completed her M.Phil in Environmental Remediation from Quaid-i-Azam University, Islamabad, Pakistan. She has recently completed her M.Phil thesis project that focuses photocatalytic treatment of dye contaminated wastewater. She obtained her BS honors (2010) in Environmental Sciences from Lahore College for Women University, Lahore, Pakistan. Her main research interests include applications of photocatalytic techniques for the remediation of environmental contaminants.

Imran Majeed is currently doing his Ph.D at Department of Chemistry, Quaid-i-Azam University Islamabad, Pakistan. His Ph.D project is about hydrogen production from renewables using visible light active  $\text{TiO}_2$  based photocatalysts. He completed Masters (2005) in Applied Chemistry from University of Engineering and Technology, Lahore, Pakistan and M.Phil (2008) in Analytical/Inorganic Chemistry from the same University. Before starting his Ph.D, he was been working as Senior Scientist in Pakistan Atomic Energy Commission, Islamabad, Pakistan.

1974, Ecological and Toxicological Association of the Dyestuffs Manufacturing Industry (ETAD) was formed with an aims to protect consumers by preventing and reducing environmental damages by fully cooperating with government over the concerns related to the toxicological impact of their own products.<sup>13</sup> In an ETAD survey, of all 4000 tested dyes, 90% dyes were found to be having their LD<sub>50</sub> values greater than  $2 \times 10^3$  mg kg<sup>-1</sup>. Among all tested dyes diazo, direct and basic dyes showed the highest rates of toxicity.<sup>14</sup>

Bright coloured dyes such as reactive and acid dyes are water soluble and the most problematic dyes to remove.<sup>15</sup> Conventional and municipal aerobic treatment systems have been proved to be ineffective on both type of dyes.<sup>16,17</sup> Compared to other types of dyes, reactive dyes are least taken up by the fabric during dyeing process, implying that the remaining quantity of dye is directly lost into the wastewater.<sup>18</sup> Leena and Raj<sup>19</sup> reported that reactive dye effluent possess the ability to remain stable and unaffected in environment for several years *i.e.* hydrolyzed reactive blue 19 has a half-life of about 46 years. Dispersed dyes do not ionize in an aqueous medium enhancing

---

*Riffat Naseem Malik is currently an Associate Professor as well as Chairperson of Department of Environmental Sciences, Quaid-i-Azam University Islamabad, Pakistan. Before this, she worked as Post-Doctoral Research Fellow (2001–2003) at Lancaster Environmental Centre, Lancaster University, UK. She has completed her Ph.D in Environmental Biology from The Reading University, Reading, UK. She had received Research Fellowship from Department of Geography, University of Turku, Finland after completing her M.Phil and M.Sc from Quaid-i-Azam University, Islamabad, Pakistan. She is the author and co-author of more than 90 scientific publications.*

*Hicham Idriss is currently working at CRI-KAUST, Saudi Basic Industries Corporation, Thuwal, Saudi Arabia as Chief Scientist. Formerly, he worked as Aberdeen Energy Futures Chair and Professor of Chemistry at the University of Aberdeen and Robert Gordon University, UK from 2008 to 2010. He is also Adjunct Professor at the Department of Chemical Engineering, Louisiana State University in the USA. Prior to 2008 he was Associate Professor at the Department of Chemistry, the University of Auckland in New Zealand where he worked for 13 years. He served as a member of the New Zealand National Energy Panel who delivered the 2020 Energy report to the New Zealand Government in 2008. He has obtained his B.Sc (1984), M.Sc (1985), Ph.D (1987) and habilitation (1997) from the University of Strasbourg in France and has postdoctoral and research associate positions at the University of Delaware and University of Illinois, Urbana (USA). He is the author and co-author of over 140 scientific papers and has served/is serving at the editorial board of scientific journals including Applied Catalysis A, Catalysis Today and Catalysis Survey from Asia. His main interest in surface science and catalysis is on metal oxides and their interface with transition metals at the fundamental and applied levels.*

their ability to bioaccumulate in aquatic living organisms.<sup>20</sup> Currently concerns related to the dye effluents are arising as many dyes are synthesized by known carcinogens such as aromatic compounds and benzidine.<sup>20</sup>

Chung *et al.*<sup>21</sup> have illustrated the dye reduction in the intestinal environment, that resulted into the formation of toxic amines. Moreover, azo dyes are readily reduced into the aromatic amines that are potentially hazardous as a result of anaerobic treatment conditions.<sup>22–25</sup>

In addition to dye pollution, in textile industries processing prior to dying procedure such as mercerization, scouring, sizing and bleaching results into the production of bleaching as well as scouring agents. However, amongst all of above mentioned concerns, colour removal from wastewater is the most complex and difficult task.<sup>18</sup> Dyes are usually the first contaminant to be recognized in industrial wastewater due to their high visibility even in minute concentrations (<1 ppm).<sup>26</sup> These coloured wastewaters are a considerable source of eutrophication as well as non-aesthetic pollution that can produce dangerous by-products by further oxidation, hydrolysis, or other chemical reactions taking place in the wastewater phase. Apart from the toxic effects of dyes in wastewater streams, presence of dyes can cause reduced light penetration resulting in reduced photosynthetic activity thus making oxygen unavailable for biodegradation of microorganism in the water.<sup>27</sup>

Apart from the textile industry, leather tanning industry,<sup>28</sup> paper industry,<sup>29</sup> food industry,<sup>30</sup> hair colourings,<sup>31</sup> photo-electrochemical cells<sup>32</sup> and light-harvesting arrays<sup>33,34</sup> also contribute towards the presence of dyes in wastewater. Majority of dyes used in various industries are toxic and carcinogenic thus posing a serious hazard to humans as well as to marine ecosystem.<sup>35</sup> Therefore, the impact of dyes released into the environment have been studied extensively in last few years.<sup>36,37</sup>

---

*Muhammad Amtiaz Nadeem is currently an Assistant professor at Quaid-i-Azam University Islamabad. He completed Masters (2003) in Chemistry from University of the Punjab, Lahore, Pakistan and M.Phil in Analytical/Inorganic Chemistry (2006) from Quaid-i-Azam University Islamabad, Pakistan. He joined Prof. Hicham Idriss group based at University of Auckland as a Ph.D student in 2008 and in 2009 moved with him at the Energy Future Center in Aberdeen, UK, to complete his Ph.D in 2012. His Ph.D thesis has been placed in Dean, Faculty of Natural Sciences, University of Auckland theses excellence list. His thesis was also nominated for University of Auckland best thesis award for 2012. His main interest in surface science and catalysis is on metal oxides and their interface with transition metals at the fundamental and applied levels.*

This paper presents an overview of the recent research improvements targeting the degradation of various dyes by using  $\text{TiO}_2$  as a potential photocatalyst.

## Dye classification

Dyes usually have many structural varieties and their complete classification with respect to one parameter is very difficult and of no use from practical understanding point of view. However, dyes are generally divided into different groups and classes depending on their source, general dye structure and the fiber type with which they are most compatible as shown in the Fig. 1.

Among major dye categories, azo dyes are the largest group of colourants and over 50% of all the dyes used in industries are azoic dyes. *Azo dyes are characterized by double bond of nitrogen ( $-N=N-$ ), where at least one of the nitrogen atom is attached to an aromatic group (rings of naphthalene or benzene).* Moreover, they have amphoteric properties due to the presence of additional carboxyl, hydroxyl, amino or sulfoxyl functional groups. Azo dyes can behave anionic (deprotonation at the acidic group), cationic (protonated at the amino group) or non-ionic depending upon the pH of the medium.<sup>38</sup> Most notable azo dyes are: acid dyes, basic dyes (cationic dyes), direct dyes (substantive dyes), disperse dyes (non-ionic dyes), reactive dyes, vat dyes and sulfur dyes.<sup>39</sup> Dyes based on general structure can also be classified as anionic, non-ionic and cationic dyes. The anionic dyes mainly include direct acidic and reactive dyes.<sup>26</sup> Major nonionic dyes include; disperse dyes which does not ionizes in the aqueous environment and the major cationic dyes include basic and disperse dyes.<sup>38</sup>

Acidic dyes are named so as they are normally applied to the nitrogenous fibers or fabrics in inorganic or organic acid solutions. Basic dyes give cations in the solution which are generally applied to acrylic and modacrylic fibers. Direct dyes are applied in aqueous bath containing ionic salts and electrolytes that bond to fibers/fabrics by electrostatics forces.<sup>40,41</sup> Disperse dyes have low solubility in water, but they can interact with the

polyester chains by forming dispersed particles.<sup>42</sup> The wash fastness with disperse dyes varies with the type of fibers being used for dyeing purpose *i.e.* poor on acetate, excellent on polyester.<sup>38</sup> Reactive dyes are primarily utilized on cellulosic fibers, but occasionally on protein fibers and nylon as well forming covalent bond with the appropriate textile functionality.<sup>43</sup> Sulfur dyes are used on cellulosic fibers to produce dull shades such as navy, black and brown. They have excellent fastness in most areas, but fades off when exposed to chlorine. Vat dyes that works with a special chemistry having excellent fastness in all areas and especially on exposure to chlorine and bleach.<sup>44–46</sup> Further characteristics of these dyes are summarized in Table 1.

## Dye treatment strategies

Apart from their physically unpleasant nature and toxicity, ever increasing massive production rate of dyes due to increasing industrialization have led to the necessity of effective treatment.<sup>47,48</sup> Therefore, in order to treat such obvious and challenging effluents, a wide range of technologies have been tested to reduce their potential magnified impacts on environment. *Traditional physical techniques* such as activated carbon, adsorption, reverse osmosis, ultrafiltration can be used for dye removal. However, these processes simply transfer the pollutants from one to another medium causing secondary pollution. This generally requires further treatment of solid-wastes and regeneration of the adsorbent, which adds more cost to the process. *Chemical process* such as chlorination, ozonation,<sup>49</sup> adsorption on organic or inorganic matrices, precipitation, chemical oxidation processes,<sup>50</sup> advanced oxidation processes such as Fenton and photo-Fenton catalytic reactions,<sup>51</sup>  $\text{H}_2\text{O}_2/\text{UV}$  processes<sup>52</sup> and photodegradation through photocatalysis are also commonly being used for the synthetic dye removal.<sup>53</sup> However, toxic unstable metabolites as a result of most of these processes<sup>54</sup> imparts adverse effects on animal and human health.<sup>55</sup>

Biological processes involving microbiological or enzymatic decomposition<sup>56</sup> and biodegradation have also been used for dye removal from wastewaters. Moutaouakkil *et al.*<sup>57</sup> isolated Azoreductase enzyme from *Enterobacter agglomerans* having ability to grow fast on methyl red dye under aerobic condition by catalyzing reductive cleavage of azo bonds. Anaerobic conditions also facilitates<sup>58</sup> the azo bond rupture leading to the colour disappearance but result in incomplete mineralization of toxic and carcinogenic by-products.<sup>59</sup> However, it has been found that these conventional biological treatment processes are ineffective for synthetic dyes having recalcitrant nature.<sup>60,61</sup> In recent years, a broad range of synthetic dyes have been extensively studied to develop a more promising technology based on *advanced oxidation process (AOPs)* that has the ability to oxidize contaminants quickly and non-selectively.<sup>50,62,63</sup> AOPs rely on *in situ* production of highly reactive hydroxyl radicals ( $\text{OH}$ ) which can virtually oxidize any compound present in the water matrix, often at a diffusion controlled reaction speed. These radicals are produced with the help of one or more primary oxidants (*e.g.* ozone, hydrogen peroxide, oxygen) and/or energy sources (*e.g.* ultraviolet light) or catalysts (*e.g.* titanium dioxide).<sup>64,65</sup> This

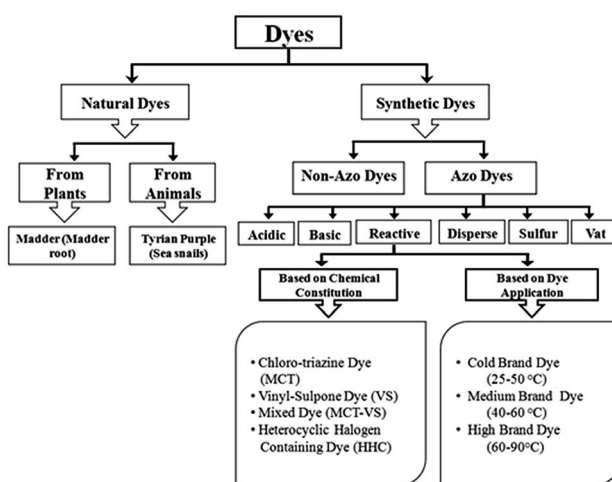


Fig. 1 Flow chart indicating dye classification on the basis of dye chemical constitution and its application.

Table 1 Types and characteristic classification of azo dyes

Dye class	Characteristics	Fiber	Dye fixation (%)	Pollutant
Acidic	Water-soluble anionic compounds	Wool, nylon, cotton blends, acrylic and protein fibers	80–93	Colour; organic acids; unfixed dyes
Basic	Water-soluble, applied in weakly acidic dye baths, very bright dyes	Acrylic, cationic, polyester, nylon, cellulosic, and protein fibers	97 and 98	NA
Direct	Water-soluble, anionic compounds, applied without mordant	Cotton, rayon and other cellulosic fibers	70–95	Colour; salts; unfixed dye; cationic fixing agents; surfactant; defoamer; levelling and retarding agents; finish; diluents
Dispersive	Insoluble in water	Polyester, acetate, modacrylic, nylon, polyester, triacetate and olefin fibers	80–92	Colour; organic acids; carriers; levelling agents; phosphates; defoamers; lubricants; dispersants; delustrants; diluents
Reactive	Water-soluble, anionic compounds, largest dye class	Cotton, cellulosic and wool fibers	60–90	Colour; salt; alkali; unfixed dye; surfactants; defoamer; diluents; finish
Sulphur	Organic compounds containing sulfur or sodium sulfide	Cotton and other cellulosic fibers	60–70	Colour; alkali; oxidizing agent; reducing agent; unfixed dye
Vat	Oldest dyes, chemically complex, water-insoluble	Cotton, wool and other cellulosic fibers	60–70	Colour; alkali; oxidizing agents; reducing agents

review focuses on mechanistic and practical aspects of dye degradation by  $\text{TiO}_2$  based photocatalysts.

## Photocatalytic dye treatment

Heterogeneous photocatalysis has proved to be as an efficient tool for degrading both atmospheric and aquatic organic contaminants.<sup>66</sup> It uses the sunlight in the presence of a semiconductor photocatalyst to accelerate the remediation of environmental contaminants and destruction of highly toxic molecules.<sup>67,68</sup> The type of the radiation used depends on the type of catalyst *i.e.* pure  $\text{TiO}_2$  works under UV light (370–415 nm). Visible light can also be used for the excitation purpose but due to unavailability of proper catalyst and other contributing factor, it has been considered as less effective source for irradiation. Generally speaking, final products of  $\text{TiO}_2$  photocatalysis have not been reported properly, which often makes evaluation of the photocatalysis difficult. The reactions of dye molecules on  $\text{TiO}_2$  photocatalysts are often confusing, and could be classified into the following categories according to the photocatalysis products. (1) Photodecolourization<sup>69–73</sup> involves simple photooxidation or photoreduction where dyes can return to the original form by either corresponding back reduction or back oxidation, respectively. (2) Photodegradation<sup>74–79</sup> involves dye decomposition to some stable products. It is the most widely used name for photocatalytic dye treatment. (3) Photomineralization<sup>80–84</sup> is regarded as complete decomposition to  $\text{CO}_2$ ,  $\text{H}_2\text{O}$ ,  $\text{N}_2$ ,  $\text{NO}_3^-$ ,  $\text{NO}_2^-$  etc. The goal of ideal photocatalysis should be mineralization. (4) Photodecomposition<sup>76,77</sup> could imply both photodegradation and mineralization differently, depending also on the researchers. However, it rarely involves decolourization. Hereafter in this

review care will be taken to use these terminologies as precisely as possible.

In order to assess the degree of dye photodegradation achieved during the treatment, generally formation of  $\text{CO}_2$  and inorganic ions is determined.<sup>81,82,85–88</sup> However, it is impossible to measure the exact concentration of these ions in case of real wastewaters. In such cases the determination of total organic carbon (TOC) or the measurement of the chemical oxygen demand (COD) or the biological oxygen demand (BOD) is used to monitor extent of dye mineralization.<sup>82,83,86,89–92</sup> In general, at lower dye concentration and for compounds which do not form stable intermediates, complete mineralization proceed with similar half-lives for parent dye and the intermediates but at higher concentration intermediates mineralization is slower than the degradation of the parent dye. To date most azo dyes have been found to undergo complete mineralization except triazine containing dyes.<sup>81–84,90</sup> The later does not undergo complete mineralization due to high stability of triazine nucleus and the stable cyanuric acid intermediates.<sup>93</sup> However, fortunately these intermediates are not toxic.<sup>80,91,92</sup> Usually COD or TOC values decrease with irradiation time whereas the amount of  $\text{NH}_4^+$ ,  $\text{Cl}^-$ ,  $\text{SO}_4^{2-}$  and  $\text{NO}_3^-$  ions increase.<sup>81,91,94</sup>

For chlorinated dye molecules,  $\text{Cl}^-$  ions are the first of the ions which appear during photocatalytic degradation.<sup>90,92,95</sup> This could be interesting in photocatalytic biological treatment which is generally not efficient for chlorinated compounds. Nitrogen is mineralized into  $\text{NH}_4^+$ ,  $\text{NO}_3^-$  and  $\text{N}_2$  depending upon initial oxidation oxidation state of nitrogen, the substrate structure and irradiation time.<sup>96,97</sup> The total amount of nitrogen-containing ions present in the solution at the end of the experiments is usually lower than that expected from stoichiometry indicating that N-containing species remain adsorbed

in the photocatalyst surface or most probably, that significant quantities of  $N_2$  and/or  $NH_3$  have been produced and transferred to the gas-phase.<sup>81,83,90</sup>

The dyes containing sulfur atoms are mainly mineralized into sulfate ions stoichiometrically.<sup>92,95</sup> Non-stoichiometric formation of sulphate ions is usually explained by a strong  $SO_4^{2-}$  adsorption on the photocatalyst surface which could partially inhibit the reaction rate.<sup>81,98,99</sup> Generally, it is found that nitrate anions have little effect on the kinetics of reaction whereas sulfate, chloride and phosphate ions, especially at concentrations of greater than  $10^{-3}$  mol  $dm^{-3}$ , can reduce the rate by 20–70% due to the competitive adsorption at the photoactivated reaction sites.<sup>98</sup>

## TiO<sub>2</sub> as dye treatment photocatalyst

Among various types of photocatalysts, titanium dioxide (TiO<sub>2</sub>) assisted photocatalytic oxidation has received much attention the last few years due to its non-toxicity, strong oxidizing power and long-term photostability.<sup>100</sup> Titanium dioxide (TiO<sub>2</sub>) is a white powder semiconductor having a wide band gap of 3.0–3.2 eV.<sup>101–103</sup> It can be excited by UV light with a wavelength below *ca.* 415 nm (in its rutile form). However, the use of TiO<sub>2</sub> is limited as only about 3–4% of the solar spectrum falls within UV range.<sup>102,104–106</sup> In general, there are three types of titanium dioxide *i.e.* anatase, rutile and brookite. In general TiO<sub>2</sub> nanoparticles are widely available commercially or can be easily prepared using sol gel method. Typically, anatase phase is often found having particle size equal to 10 nm or less with a band gap of 3.2 eV corresponding to a UV wavelength of 385 nm.<sup>107</sup> Comparatively, though some exceptions exists, rutile phase generally exists having particle size in the order of 50 nm or so.<sup>108</sup> Moreover, rutile has a smaller band gap of 3.0 eV with excitation wavelengths extending to visible 410 nm range. Thermodynamics dictates that heating the anatase phase results in gradual phase transformation of anatase to rutile and therefore depending on the method of preparation mix phase anatase-rutile can be easily prepared or purchased. For example, some commercially available TiO<sub>2</sub> that is a mixture of two phases, 80% anatase and 20% rutile, and has usually a BET area of  $50\text{ m}^2\text{ g}^{-1}$  has widely been studied.<sup>109</sup>

Most of the studies have been carried out with anatase phase due to its high photocatalytic efficiency and adsorption affinity for the organic compounds as compared to the rutile phase.<sup>110,111</sup> Shiga *et al.*<sup>112</sup> using nanocrystalline film electrodes of TiO<sub>2</sub> for photoelectrochemical activities showed that the anatase has a higher photoactivity than rutile phase at a longer wavelength. This is due to the fact that anatase phase due to its greater hole trapping ability (about 10-fold) exhibits lower recombination rates compared to rutile type.<sup>113,114</sup> Therefore, anatase is generally regarded as photochemically more active phase of TiO<sub>2</sub> due to these combined effect.<sup>107</sup> Moreover, recently developed various forms of TiO<sub>2</sub>, such as TiO<sub>2</sub> powders, TiO<sub>2</sub> film,<sup>115</sup> supported TiO<sub>2</sub>,<sup>116,117</sup> TiO<sub>2</sub> nanotubes<sup>118</sup> and doped TiO<sub>2</sub>,<sup>119,120</sup> have been evaluated through degradation of dyes and phenolic compounds. Such studies demonstrated the higher

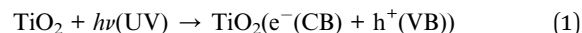
efficiency of various forms of TiO<sub>2</sub> used for removal of dyes and phenolic compounds from aqueous solutions.<sup>121</sup>

## Basic principles and mechanism for photocatalyzed dye degradation

### Indirect dye degradation mechanism

The indirect heterogeneous photocatalytic oxidation mechanism using semiconducting materials can be summarized as follows.<sup>122,123</sup>

**a. Photoexcitation.** Photocatalytic reaction is initiated when a photoelectron is promoted from the filled valence band of a semiconductor photocatalyst *i.e.* TiO<sub>2</sub> to the empty conduction band as a result of irradiation. The absorbed photon has energy ( $h\nu$ ) either equal or greater than the band gap of the semiconductor photocatalyst. The excitation process leaves behind a hole in the valence band ( $h_{VB}^+$ ). Thus as a net result, electron and hole pair ( $e^-/h^+$ ) is generated as indicated by the eqn (1) below.



**b. Ionization of water.** The photogenerated holes at the valence band then react with water to produce OH· radical.



The OH· radical formed on the irradiated semiconductor surface are extremely powerful oxidizing agent. It attacks adsorbed organic molecules or those that are very close to the catalyst surface non-selectively, causing them to mineralize to an extent depending upon their structure and stability level. It does not only easily attack organic pollutants but can also attack microorganisms for their enhanced decontamination.<sup>124</sup>

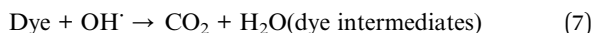
**c. Oxygen ionosorption.** While the photogenerated hole ( $h_{VB}^+$ ) reacts with surface bound water or  $OH^-$  to produce the hydroxyl radical, electron in the conduction ( $e_{CB}^-$ ) is taken up by the oxygen in order to generate anionic superoxide radical ( $O_2^-$ ).



This superoxide ion may not only take part in the further oxidation process but also prevents the electron-hole recombination, thus maintaining electron neutrality within the TiO<sub>2</sub> molecule.

**d. Protonation of superoxide.** The superoxide ( $O_2^-$ ) produced gets protonated forming hydroperoxyl radical ( $HO_2^{\cdot}$ ) and then subsequently  $H_2O_2$  which further dissociates into highly reactive hydroxyl radicals (OH).

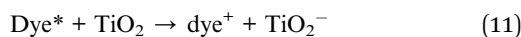




Both oxidation and reduction processes commonly take place on the surface of the photoexcited semiconductor photocatalyst. The complete process has been represented by the Fig. 2.

### Direct mechanism for dye degradation

Owing to their ability to easily absorb some of visible light, another mechanism of photocatalytic dye degradation can also occur under visible light. This mechanism involves the dye excitation under visible light photon ( $\lambda > 400$  nm) from the ground state (Dye) to the triplet excited state (Dye\*). This excited state dye species is further converted into a semi-oxidized radical cation (Dye<sup>+</sup>) by an electron injection into the conduction band of TiO<sub>2</sub>.<sup>125</sup> Due to reaction between these trapped electrons and dissolved oxygen in the system superoxide radical anions (O<sub>2</sub><sup>-</sup>) are formed which in turn result into hydroxyl radicals (OH<sup>-</sup>) formation. These OH<sup>-</sup> radicals are mainly responsible for the oxidation of the organic compounds represented by the equations and Fig. 3 below.<sup>126-128</sup>



According to many studies, indirect mechanism is generally prevalent over direct mechanism and its contribution to the dye degradation is much more pronounced than the visible light initiated mechanism. The latter is believed to be a far slower reaction compared to indirect mechanism.<sup>126,129</sup>

## Factors affecting photocatalytic dye degradation

### Effect of pH

The pH is one of the significant parameters for the photocatalytic dye degradation as it can influence dye reaction rates in multiple ways as explained here on. It can influence dye adsorption onto the semiconductor surface<sup>121</sup> as catalyst surface charge depends on the pH of a given solution. Zhu *et al.*<sup>130</sup>

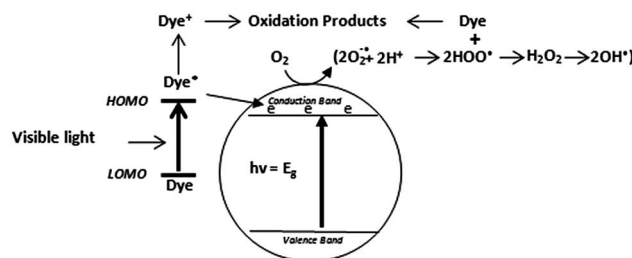


Fig. 3 Pictorial representation of direct dye degradation process.

demonstrated that pH effect is related to the surface-charge properties of the photocatalysts, and could be explained on the basis of point of zero charge (PZC). The point of zero charge for TiO<sub>2</sub> particles is pH<sub>PZC</sub> = 6.8.<sup>3</sup> At a pH values lower than pH<sub>PZC</sub> (pH < 6.8) or at acidic solution, the surface of the catalyst gets positively charged and *vice versa*<sup>131,132</sup> according to the eqn (12) and (13) given below.



When the pH is lower than the PZC value the adsorbent surface is positively charged and the surface becomes anions attracting/cation repelling. Conversely, above PZC the surface is negatively charged and the surface becomes cation attracting/anion repelling.

Zhu *et al.*<sup>130</sup> explained that highest degree of decolourization of methyl orange observed at pH 2 is attributed to the electrostatic attraction between the positively charged catalyst surface and methyl orange anions, which led to the increase in degree of adsorption and 97% photodecolourization. However, the dye treatment results based on dye adsorption strength cannot be explained as there are many other parameters operating at the same time. For example, Muruganandham *et al.*<sup>133</sup> found that increasing pH from 1 to 9 increased decolourization rates for reactive orange 4 (an anionic dye) from 25.27% to 90.49% after 40 min and degradation from 15.16% to 87.24% within 80 minutes, respectively. However, the faster rate of color removal and photodegradation was observed at alkaline pH. In contrast, the degradation studies of some azo dyes showed conflicting results.<sup>134</sup> For example, acid yellow 17 (an anionic dye) has shown to be more degraded at pH 3, whereas, orange II (anionic dye) and amido black 10B (anionic dye) showed maximum degradation at pH 9.<sup>135</sup>

The pH can also affect whole photocatalytic dye degradation mechanism and thus the degradation rate. For example positive holes generated at lower pH act as major oxidation species, however at higher or neutral pH range, hydroxyl radicals (OH<sup>-</sup>) are largely responsible for oxidation process.<sup>136</sup> On one hand, these radicals can be generated in an alkaline solution,<sup>137</sup> however, on the other hand sites the semiconductor surface may not adsorb dye anions due to electrostatic repulsion thereby decreasing their degradation and *vice versa*.<sup>138</sup> It is believed that hydroxyl radicals play an essential role in the fission of the -N=N- conjugated system in azo dyes in a TiO<sub>2</sub>

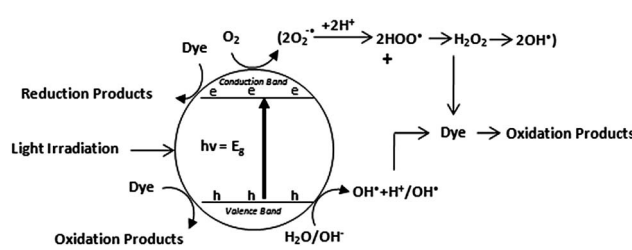


Fig. 2 Pictorial representation of indirect dye degradation process.<sup>24</sup>

assisted photodegradation. The azo linkage ( $-N=N-$ ) is mainly vulnerable to electrophilic attack by hydroxyl radical. Riga *et al.*<sup>109</sup> reported that dye decolourization and degradation rate increases with increasing pH. Whereas, at lower pH the concentration of  $H^+$  exceeds and these  $H^+$  ions interact with azo linkage reducing the azo group electron densities, resulting into decrease in hydroxyl reactivity of hydroxyl radicals by electrophilic mechanism.

It has been reported that a dye with positive charge shows higher adsorption rate on an unmodified  $TiO_2$  than for dyes with a negative charge (anionic).<sup>139</sup> It has been studied that titanium dioxide has a higher oxidizing activity at lower pH; however, excess of  $H^+$  at very low pH can decrease the rate of reaction too. This can be explained by the characteristic of  $TiO_2$  particles that tend to agglomerate at lower or acidic condition, which may reduce surface area of catalyst for maximum dye adsorption as well as photon absorption.<sup>121,140,141</sup> Bizani *et al.*<sup>142</sup> reported that the pH effect on dye degradation rate can be explained mainly by the modification of the electrical double layer of the solid-electrolyte interface, which consequently affects the sorption-desorption processes and the separation of the photogenerated electron-hole pairs on the surface of the semiconductor particles.<sup>142</sup>

### Effect of pollutant adsorption strength

In heterogeneous photocatalysis, competitive adsorption between water molecules and the target molecules that are to be degraded plays an important role in photocatalysis.<sup>143,144</sup> This is due to the fact that photogenerated oxidizing species may not migrate far away from their formation centres resulting into negligible or a very slow rate of degradation at few nanometer layers around the catalyst particles surface.<sup>145</sup> However, in various studies many authors have not reported a direct relationship between adsorption and photodegradation. In some cases, adsorption of compounds or intermediates may acts as poison on the catalyst surface. Vautier *et al.*<sup>146</sup> reported that an electrostatic interactions between the dye molecule and the hydroxyl groups of the photocatalyst is always required for proper dye adsorption.

Bizani *et al.*<sup>142</sup> reported that strong adsorption may lead to a multilayer of dye molecules around the catalyst particles surface. This may result into limited interaction between excited dye molecule and the catalyst in case of direct degradation mechanism or between incoming light and the catalyst in case of indirect mechanism. In both of above cases the photooxidation process is expected to decrease. This could be the reason due to which the initial decolourization rate of the dye is reported lower in acidic solutions. On the other hand, in alkaline solutions, decrease in the initial rate of degradation reflects the difficulty of the anionic dye molecules to approach the catalyst surface.<sup>147-149</sup>

### Effect of light intensity

Band-gap sensitization mechanism does not have any influence on photocatalytic degradation rate or mechanism.<sup>101</sup> However, various studies have revealed that with an increasing light

intensity, the rate of photocatalytic degradation increases.<sup>150-152</sup> Collazzo *et al.*<sup>153</sup> compared the direct black 38 dye degradation ability of nitrogen doped  $TiO_2$  under visible light source and sunlight. It was confirmed that nitrogen doped  $TiO_2$  due to its higher absorption in visible region showed higher dye degradation (60% in 6 hours) under visible light. Under sunlight irradiation, N-doped  $TiO_2$  exhibited degradation efficiency slightly higher than non-doped  $TiO_2$  as shown in Fig. 4.

### Effect of photocatalyst load

In order to avoid the excess use of the catalyst, it is necessary to calculate optimum dose or loading of the catalyst for efficient removal of dye. Of course the amount of catalysts required will depend on the configuration of the reactor, light intensity, type of the targeted dye and the type as well as particle morphology of the catalyst. Owing to these many contributing factors there are inconsistencies in the optimum catalyst dose used by different researchers. Several authors have investigated the function of catalyst loading on the reaction rate of photocatalytic oxidation process.<sup>133,154-156</sup> Riga *et al.* reported that the amount of dye adsorbed on catalyst surface generally increases by increasing the  $TiO_2$  loading or the catalyst used. It was found that generally  $TiO_2$  loading increases rate of photodecolourization, especially up to  $1000\text{ mg L}^{-1}$  with an overall 60% TOC removal rate.<sup>109</sup>

Kaur *et al.*<sup>102</sup> reported that in all of the optimized conditions of efficiency, the catalyst dose for maximum photocatalytic degradation of reactive red 198 is  $0.3\text{ g L}^{-1}$ . However, in another study, the optimized condition for  $TiO_2$  consumption was stated to be  $0.5\text{ g L}^{-1}$ .<sup>157</sup> Mahvi *et al.*<sup>138</sup> studied that an increase in the amount of catalyst to the level constant with the optimized level of light absorption (normally  $0.4\text{ g L}^{-1}$ ), increases the amount of the decolourization.<sup>157-159</sup> Also, Muruganandham *et al.*<sup>133</sup> reported that an increase of catalyst weight from  $1.0\text{ g L}^{-1}$  to  $4.0\text{ g L}^{-1}$  increases the dye decolourization sharply from 69.27% to 95.23% at 60 minutes and dye degradation from 74.54% to 97.29% at 150 min. A similar observation has been made by other authors, as well.<sup>137,148,160</sup>

It is evident that initially photodegradation rate increases with an increase in the amount of photocatalyst and then decreases with increase in catalyst concentration (Fig. 5). This trend can be explained by three possibilities:

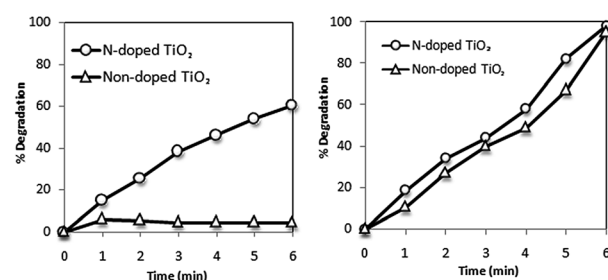


Fig. 4 Photocatalytic degradation of direct black 38 as a function of time under visible light (left) and sunlight (right). Experimental conditions:  $C_0 = 0.055\text{ g L}^{-1}$ ,  $C_{\text{catalyst}} = 1.0\text{ g L}^{-1}$ ,  $pH = 2.5$ ,  $T = 25\text{ }^\circ\text{C}$ .<sup>153</sup>

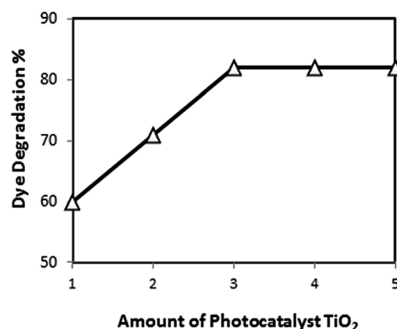


Fig. 5 Effect of increasing  $\text{TiO}_2$  catalyst loadings (in grams) on rate of dye degradation.<sup>141</sup>

1 When all dye molecules are adsorbed on photocatalyst surface, the addition of higher quantities of photocatalyst would have no further enhancing effect on the degradation efficiency.

2 Another possible reason could be due to the fact that an excess of photocatalyst particles may increase opacity of the suspension which may retard the degradation rate.<sup>161</sup> Zhu *et al.*<sup>130</sup> reported in their study that as the amount of photocatalyst was increased from  $0.05$  to  $0.5 \text{ g L}^{-1}$  the number of absorbed photons increased indicating  $97\%$  photocatalytic decolorization of methyl orange solution. However, it was found that at photocatalyst dosages above  $0.5 \text{ g L}^{-1}$ , the rate constants decreased due to the blocking of light penetration by the excessive amount of photocatalysts.<sup>162</sup>

3 Moreover, particle–particle interaction becomes significant as the amount of particles in solution increases. This may result in an enhanced rate of deactivation of activated molecules by collision with ground state titanium dioxide particles and hence decreases in dye concentration.<sup>141,163</sup>

### Effect of the initial dye concentration

It has been reported earlier that by increasing the dye concentration, the decolourization rate constant ( $k$ ) decreases.<sup>138</sup> The initial dye concentration can affect the rate of photodegradation based upon two main aspects.

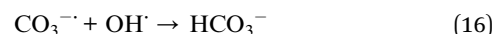
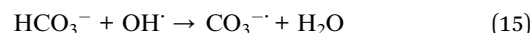
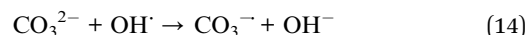
(1) In high dye concentrations, more active sites may be covered with dye ions. This further may lead to the decrease in the production of OH radicals on the surface of catalyst. Illinois *et al.*<sup>164</sup> studied the influence of various initial dye concentrations for reactive yellow 125 dye on the photocatalytic discolouration and degradation in the concentration range of  $0.025$ – $0.1 \text{ g L}^{-1}$ . They concluded that increasing the dye concentration will render the process less efficient by decreasing degradation efficiency.

(2) Zhu *et al.*<sup>130</sup> reported that the path length of the photons entering the solution decreases as the initial concentration of methyl orange increased. The reversal occurred for the lower concentration, thereby increasing the number of photons absorbed by the catalyst.<sup>132</sup> The same {Zhu, 2005 #167} effect was reported by Wang *et al.*<sup>165</sup> during their study of the photocatalytic degradation of commercial dyes using zinc oxide power as photocatalyst.

### Effect of inorganic salts

The presence of mineral ions in dye contents of wastewater is common. Some cations such as copper, phosphate and iron have been reported to have the ability to decrease the photodegradation efficiency present in certain concentration. One of the major reasons is that these substances may compete with dyes for the active sites on the  $\text{TiO}_2$  surface and thus deactivate the photocatalyst resulting in decreased degradation of targeted dyes. Whereas calcium, magnesium and zinc have been studied to have little effect on the photodegradation of organic compounds which is associated to the fact that these cations are present in their highest oxidation states causing no inhibitory effect.<sup>166</sup>

The dye industry wastewater contains a considerable amount of inorganic anions such as carbonates, chlorides, nitrate, and sulphates. The presence of these salts causes colloidal instability, increases mass transfer and decrease in the surface contact between the target dye molecule and the photocatalyst.<sup>166</sup> Degradation of dyes decreases in the presence of these ions. These  $\text{CO}_3^{2-}$  and  $\text{HCO}_3^-$  ions may scavenge the  $\text{HO}^\cdot$  radicals.<sup>24</sup>

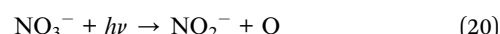


The decrease in degradation efficiency in the presence of chloride ion is due to the hole scavenging properties of chloride ion.



The chloride radical anions formed can also block the active sites of the catalyst surface. The inhibitory effect of chloride and phosphate ions on the photocatalytic degradation has also already been reported.<sup>167</sup> The inhibiting effect of  $\text{CO}_3^{2-}$  ion is greater than the inhibiting effect of  $\text{Cl}^-$  ion.

Wang *et al.*<sup>168</sup> reported the effect of  $\text{NO}_3^-$  and  $\text{SO}_4^{2-}$  on the photodegradation of reactive red 2 dye under UV irradiation, stating an increased in dye removal. Zhu *et al.*<sup>169</sup> also reported the same results that the presence of  $\text{NO}_3^-$  accelerated the photocatalytic degradation of an azo dye under visible light irradiation in their experiment. This can be attributed to the direct or indirect hydroxyl radical formation as follow:



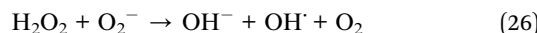
$\text{SO}_4^{2-}$  in photocatalytic dye degradation has two important roles.  $\text{SO}_4^{2-}$ , by driving the dye molecule to bulk interface, increases aqueous ionic strength that results into enhanced photocatalytic efficiency. Also, the adsorbed  $\text{SO}_4^{2-}$  reacts with generated valence band holes forming  $\text{SO}_4^-$ . This reaction between  $\text{SO}_4^{2-}$  and photogenerated  $h_{\text{VB}}^+$  on the photocatalyst surface can prevent the electrons and holes recombination, enhancing photodegradation rate as:



$\text{SO}_4^-$  is a very strong oxidant with redox potential of +2.6 V, which can enhance dye degradation. Further, the degradation rates also depend on type of salt used. This effect has been studied by various authors.<sup>109,133,138,170-172</sup>

### Effect of addition of oxidizing species

Addition of powerful oxidizing species, such as hydrogen peroxide ( $\text{H}_2\text{O}_2$ ) and potassium peroxydisulfate ( $\text{K}_2\text{S}_2\text{O}_8$ ) to  $\text{TiO}_2$  suspensions is a well-known procedure which increases rate of photooxidation.<sup>47,95,148,160,173</sup> Hydrogen peroxide is believed to have a dual role during the process of photocatalytic degradation. It accepts an electron from the conduction band, thus, promotes the charge separation and it also forms OH radicals.



At  $\text{H}_2\text{O}_2$  concentration greater than critical concentration, it may act as hole or  $\text{OH}^-$  scavenger or react with  $\text{TiO}_2$  to form peroxy compounds, which are detrimental to the photocatalytic action.<sup>148,174-177</sup> Bizani *et al.*<sup>142</sup> reported that the addition of oxidants such as  $\text{H}_2\text{O}_2$  appears to be more effective in photocatalytic degradation of dyes than  $\text{K}_2\text{S}_2\text{O}_8$  comparatively, although their effectiveness in decolorizing the solutions can be reversed. Dye intermediates showed higher toxicity values involving  $\text{K}_2\text{S}_2\text{O}_8$  than photocatalytic process involving  $\text{H}_2\text{O}_2$ , indicating partial DOC (dissolved organic carbon) and toxicity removal efficiency.

## Strategies for enhancing photocatalytic properties of $\text{TiO}_2$

### Photocatalysis by adopting advanced oxidation procedures

Recently cavitation methods have attracted attention as AOPs for the removal of carcinogenic chemicals present in water.<sup>178,179</sup> Cavitation involves the growth, nucleation and implosive collapse of micro-bubbles and cavities that occur in fractions of microseconds, releasing large amount of energy over a small location that behave as micro-reactors.<sup>168</sup> In acoustic cavitation, pressure variations in liquid are effected through sound waves (16 kHz to 100 MHz) using ultrasonic transducers as represented in Fig. 6. This produces oscillating bubbles of various size moving at different velocities.<sup>180</sup> The motion of the bubbles

and their radial pulsation can be controlled by acoustic field in the resonating system.<sup>181</sup> It has been observed that enhancement due to such synergistic mechanism is due to the deagglomerating effect of photocatalyst through ultrasound, resulting into increased surface area and catalytic performance.<sup>182-185</sup> However, industrial application of ultrasonically induced cavitation is a problem due to ineffective distribution of the cavitation activity on a large scale.<sup>186,187</sup> Wang *et al.*<sup>168</sup> studied the efficiency of combined treatment in which they used photocatalysis and water jet cavitation on reactive red 2 dye degradation. The results showed a significant enhancement of photocatalytic activity up to *ca.* 136%.

In hydrodynamic cavitation, cavitation is produced by pressure variations obtained by creating velocity variation and decrease in static pressure that occurs when the fluid passes through a constriction.<sup>188</sup> Saharan *et al.*<sup>189</sup> reported that hydrodynamic cavitation is more energy efficient compared to acoustic cavitation and has a higher degradation as for equivalent power/energy dissipation. In addition, other AOTs including organic contaminants degradation using  $\text{SO}_4^-$  have recently been introduced.<sup>190-193</sup> These include radiolytic or photolytic or thermal activation of persulfate or peroxide bond to break it down to produce  $\text{SO}_4^-$ .  $\text{SO}_4^-$  showed a higher reduction potential of 2.5–3.1 V as compared with  $\text{OH}^-$  having a standard reduction potential of 1.8–2.7 V. Moreover, it is more selective for the oxidation of organic contaminants over a wide range of pH.<sup>194,195</sup> In addition,  $\text{SO}_4^-$  have a longer half-life, depending on its preference for reactions related to electron transfer, whereas  $\text{OH}^-$  with an equal preference participates in every reaction.<sup>172,194,196</sup>

### Development of efficient $\text{TiO}_2$ photocatalysts by doping

There are various research studies on photocatalytic degradation of dyes using  $\text{TiO}_2$  in several modified forms for performance enhancement under visible light. These include adsorption and surface complexation on  $\text{TiO}_2$ , non-metal doping, lanthanide ion doping, transition metal doping, noble metal doping and multi-atom doping. The main purpose of doping is to decrease the band gap of pure  $\text{TiO}_2$  (3.2 eV for

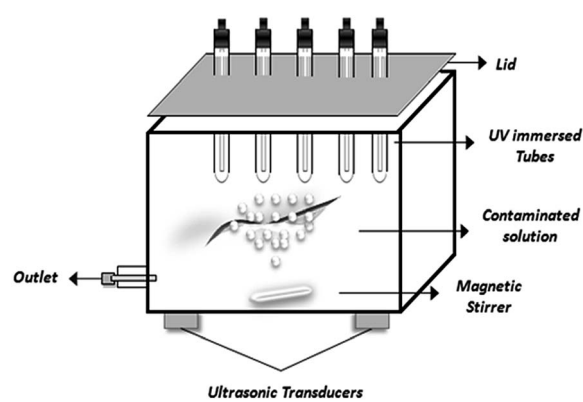


Fig. 6 Application of cavitation technology to photocatalysis by using ultrasonic transducers for efficient treatment of organic contaminants.

anatase phase) to bring the absorption band from UV to visible region. The Fig. 7 below represents the simplified and relative band position and band gap of pure, metal and non-metal doped  $\text{TiO}_2$ . The details about the doping methodologies and photocatalysis mechanisms can be found elsewhere.<sup>197-199</sup>

### Non-metal doping

There are various reports available on non-metal doping of  $\text{TiO}_2$ , especially with boron,<sup>200</sup> carbon,<sup>201</sup> sulfur, nitrogen and fluorine.<sup>202</sup> The main objective of non-metal doping is to bring the absorption band of  $\text{TiO}_2$  to visible region. Apart from its advantages, however, long-term instability of the photocatalyst is a major drawback.<sup>202</sup> The detail about the dye degradation including nitrogen and carbon doped  $\text{TiO}_2$  is given below under separate headings.

**Nitrogen doping.** The nitrogen-doped  $\text{TiO}_2$  photocatalysts have been tested for the decomposition of aqueous solutions of organic compounds and dyes under UV and visible light illumination.<sup>201,203-207</sup> Some examples of the N-doped  $\text{TiO}_2$  catalysts used for different dye degradation studies along with their preparation technique are given in Table 2.

Asahi *et al.* and others reported that nitrogen due to its comparable size and electronegativity to that of oxygen is the most suitable element for reducing the band gap width of  $\text{TiO}_2$ .<sup>216,217</sup> Irie *et al.*<sup>218</sup> proposed that an isolated narrow band formed above the valence band in  $\text{TiO}_{2-x}\text{N}_x$  powder is responsible for the visible light response. In addition, increasing nitrogen concentration lowered the quantum yield under UV illumination, indicating that the doping sites could also work as recombination centers. Parida and Naik<sup>219</sup> reported the degradation of methylene blue and methyl orange using N-doped  $\text{TiO}_2$  showing 67% and 59% of degradation after 4 hours irradiation under visible light source. Selvaraj *et al.*<sup>220</sup> measured the photocatalytic degradation of the reactive triazine dyes including reactive yellow 84, reactive red 120 and reactive blue 160 on N-doped  $\text{TiO}_2$  anatase and P25 in the presence of natural sunlight. It was reported that reactive yellow 84 indicated a faster degradation on N-doped  $\text{TiO}_2$  in sunlight than the commercial Aerioxide P25. However, the P25 indicated higher photocatalytic activity for the other two dyes. The COD level within 3 h sunlight exposure, reduced to 65.1, 73.1, and 69.6% for reactive yellow-84, reactive red 120 and reactive blue 160 respectively. In two separate studies, Ihara *et al.*<sup>221</sup> and

Serpone<sup>222</sup> argued that synthesized nitrogen doped  $\text{TiO}_2$  with the sites that were oxygen deficient formed in the grain boundaries were responsible for the visible light response, whereas presence of nitrogen had only enhanced the stabilization of these oxygen vacancies. Songkhum and Tantirungrotechai<sup>223</sup> prepared nitrogen and iron(III) co-doped  $\text{TiO}_2$  ( $\text{N-Fe-TiO}_2$ ) and reported active for the photodegradation of methyl orange. However, corresponding to the absorption spectra the synthesized  $\text{TiO}_2$  photocatalysts except, under UV irradiation, were not found to be photocatalytically active under visible light irradiation. In summary, it can be concluded that, apart from vague understanding of dye degradation mechanism under visible light and various disadvantages, use of nitrogen doped  $\text{TiO}_2$  may outweigh non-doped  $\text{TiO}_2$  in near future due to its dye degradation activity under practically available sunlight.<sup>224</sup>

**Carbon doping.** In recent years, dopants such as carbon and nitrogen have received more attention owing to their low cost with demonstration of narrow band gap which results in significant visible light absorption capability.<sup>225</sup> Different routes have been developed to synthesize carbon doped  $\text{TiO}_2$  which can broadly be divided into two categories *i.e.* inner and outside synthetic route. Inner approach includes incorporation of carbon into  $\text{TiO}_2$  structure during its synthesis while outside approach includes the incorporation after  $\text{TiO}_2$  has already been synthesised. Khan *et al.*<sup>226</sup> manufactured carbon doped  $\text{TiO}_2$  by controlled combustion of Ti metal in a natural gas flame. Irie *et al.*<sup>218</sup> prepared carbon doped anatase  $\text{TiO}_2$  nanoparticles by oxidative annealing of  $\text{TiC}$  under  $\text{O}_2$  flow at 873 K. Sakthivel and Kwasch<sup>227</sup> synthesized carbon-doped  $\text{TiO}_2$  nanoparticles by hydrolysis of  $\text{TiCl}_4$  with tetrabutylammonium hydroxide followed by calcination of the precipitate obtained as a result of wet process.

Ren *et al.*<sup>228</sup> prepared doped  $\text{TiO}_2$  using outside preparation approach. They added required amounts of amorphous  $\text{TiO}_2$ , glucose, deionized water in a Teflon lined stainless steel autoclave by marinating the temperature at 160 °C for 12 hours.

Velmurugan *et al.*<sup>229</sup> recently synthesized carbon nanoparticle loaded  $\text{TiO}_2$  (CNP- $\text{TiO}_2$ ) through sonochemical method. CNP- $\text{TiO}_2$  was found to be stable and reusable. Comparatively, photocatalytic activity of CNP- $\text{TiO}_2$  under solar light for degradation of reactive red 120 was found higher than  $\text{TiO}_2$  P-25 and as prepared  $\text{TiO}_2$ . Increase in activity was related to suppression in recombination of photogenerated electron-hole pair by loaded CNP indicated by a decrease of measured photoluminescence intensity.

### Lanthanide ions doping

Lanthanide ions are known for their complex formation with various Lewis bases *e.g.* aldehydes, acids, amines, alcohols, thiols. These Lewis bases interact with the f-orbitals of the lanthanides through their functional groups. Thus, incorporation of lanthanide ions into a  $\text{TiO}_2$  matrix could provide a mean to concentrate the organic pollutant at the semiconductor surface and consequently enhance the photoactivity of  $\text{TiO}_2$ .<sup>230-232</sup> It has been reported in literature that the optimum

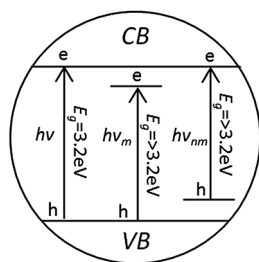


Fig. 7 Simplified relative energy band positions and band widths for pure ( $h\nu$ ) metal doped ( $h\nu_m$ ) and non-metal doped ( $h\nu_{nm}$ )  $\text{TiO}_2$  anatase.<sup>197</sup>

Table 2 Studies on N-doped TiO<sub>2</sub> assisted photodegradation of different dyes

Catalyst	Dyes used for analysis	Techniques for preparation of N-doped TiO <sub>2</sub> catalysts	Ref.
N-Doped TiO <sub>2</sub>	Rhodamine B	Microemulsion-hydrothermal method	208
N-Doped anatase and rutile	Methyl blue	Calcination of acidified TiCl <sub>3</sub> in presence of urea and oxalic acid	209
N-Doped TiO <sub>2</sub> nanotubes	Methyl orange	Solvothermal process	210
Microarrays of N-doped flower-like TiO <sub>2</sub>	Methyl orange	Electrochemical anodization of Ti in NH <sub>4</sub> F aqueous solution	211
N-TiO <sub>2</sub>	Methyl orange and phenol	Microwave method	212
N-TiO <sub>2</sub> nano colloid	Methyl blue	Nitridation of a porous TiO <sub>2</sub>	213
N-TiO <sub>2</sub>	Ethyl blue and 4-chlorophenol	Sol gel using NH <sub>4</sub> Cl as nitrogen source	207
N-TiO <sub>2</sub>	Methyl blue	Simple method	214
N-TiO <sub>2</sub>	Rhodamine B	Plasma based ion implantation	215

level of rare earth metal doping is 1–2% to hinder the crystal growth of TiO<sub>2</sub> during calcinations.<sup>202</sup> Although doping of lanthanide ions into TiO<sub>2</sub> attracted some attentions still such works are little so far. Additionally, lanthanides ions can in fact trap conductive band electrons when restricted to the TiO<sub>2</sub> surface.<sup>233</sup> Recently, La<sup>3+</sup>, Nd<sup>3+</sup>, Sm<sup>3+</sup>, Eu<sup>3+</sup>, Gd<sup>3+</sup>, and Yb<sup>3+</sup> modified TiO<sub>2</sub> nanoparticles with their ability to increase the anatase phase stability and preventing the segregation of TiO<sub>2</sub> have excessively been investigated for maximizing the efficiency of photocatalytic reactions.<sup>234–236</sup> Xie *et al.*<sup>237,238</sup> prepared three types of lanthanide ion-modified titanium dioxide *i.e.* Eu<sup>3+</sup>–TiO<sub>2</sub>, Nd<sup>3+</sup>–TiO<sub>2</sub> and Ce<sup>4+</sup>–TiO<sub>2</sub> and tested for the photodegradation of azo dye X–3B under visible light irradiation. The results showed that Ln<sup>n+</sup>–TiO<sub>2</sub> system had a higher photocurrent generation. They ranked reaction rates as Nd<sup>3+</sup>–TiO<sub>2</sub> sol > Eu<sup>3+</sup>–TiO<sub>2</sub> sol > Ce<sup>4+</sup>–TiO<sub>2</sub> sol > TiO<sub>2</sub> sol > P-25 TiO<sub>2</sub> powder. Zhang *et al.*<sup>239</sup> prepared TiO<sub>2</sub> particles co-doped with boron and lanthanum (B–La–TiO<sub>2</sub>) at a molar ratio of 1 : 4 and investigated their photocatalytic performance to photodegrade methyl orange dye. The result showed organic dye degradation to 98% within 90 min compared to 24% with undoped TiO<sub>2</sub>. It was speculated that the reason behind enhanced photocatalytic activity of B–La–TiO<sub>2</sub> photocatalysts is its excellent photocatalytic effect under the visible light region.

Very recently, Lan *et al.*<sup>240</sup> successfully prepared lanthanum and boron co-doped TiO<sub>2</sub> (La–B–TiO<sub>2</sub>) by modified sol–gel method to enhance the visible-light photocatalytic performance by improving the quantum efficiency of the photocatalytic reaction. 1% La–B–TiO<sub>2</sub> catalysts showed highest photocatalytic degradation of acid orange 7 up to 93% under visible-light irradiation for 5 h. Nasir *et al.*<sup>241</sup> synthesized 0.1 Ce/C co-doped TiO<sub>2</sub> *via* hydrothermal method for the efficient degradation of an aqueous solution of acid orange 7 dye under visible light irradiation. Co-doped catalysts showed higher photocatalytic activity compared to C-doped catalyst. However, increasing Ce concentration above 0.1 Ce/C–TiO<sub>2</sub> resulted in an increase of electrons and holes recombination. In another study Nasir *et al.*<sup>242</sup> again used Ce to prepared Ce–S co-doped TiO<sub>2</sub> because of its Ce<sup>3+</sup>/Ce<sup>4+</sup> redox couple, which contains the ability to shift between Ce<sub>2</sub>O<sub>3</sub> and CeO<sub>2</sub> under reducing and oxidizing conditions.<sup>243</sup> Results indicated that decrease in the particle size, increase in the surface area, abundance of surface hydroxyl

groups, and reduction of recombination of e<sup>–</sup> and h<sup>+</sup> assisted the enhanced photocatalytic degradation of acid orange dye.

### Transition metal doping

Incorporating transition metals in the TiO<sub>2</sub> crystal lattice may result in the formation of new energy levels between valence and conduction band, inducing a shift of light absorption towards the visible light region. However, it has been reported as well that transition metals may cause thermal instability for the anatase phase of TiO<sub>2</sub>.<sup>244</sup>

**Cadmium doping.** Cadmium is one of the heavy metals which could be present in real dyes containing wastewater. It can modify the photocatalytic activity of the catalyst by being absorbed on the photocatalyst surface.<sup>245</sup> Andronic *et al.*<sup>245</sup> investigated the photocatalytic efficiency of cadmium doped TiO<sub>2</sub> thin films obtained using the doctor blade deposition method to degrade methyl orange and methylene blue dyes. Results showed a linear correlation between the band gap energy of the cadmium doped TiO<sub>2</sub> films and dyes photodegradation efficiency. Some authors have reported negative or overall no effect of cadmium ion on the photocatalytic activity.<sup>246</sup> However, these effects highly depend on the cadmium concentration and doping method used. More studies are needed to understand the system completely as Cd may be oxidized to CdO which is a *p*-type semiconductor thus modifying the electronic properties of the system.

**Copper doping.** It has been reported that Cu(II) has the ability to extend the light absorption to visible region by modifying the TiO<sub>2</sub> valence band spectrum resulting into improved photocatalytic activity.<sup>247–249</sup> Copper sulphides have also largely been investigated in recent years due to their remarkable optical and electrical properties as a result of variations in composition, morphology, stoichiometry and their potential applications as absorbers for solid state solar cells.<sup>250,251</sup> Andronic *et al.*<sup>252</sup> studied the photocatalytic process by using Cu<sub>x</sub>S and coupled Cu<sub>x</sub>S/TiO<sub>2</sub> thin films for methyl orange and methylene blue photodegradation. The photocatalytic activity of Cu<sub>x</sub>S/TiO<sub>2</sub> nanocomposites depended on Cu<sub>x</sub>S : TiO<sub>2</sub> ratio. The best results were achieved under UV irradiation, when H<sub>2</sub>O<sub>2</sub> is added in photocatalytic process at Cu<sub>x</sub>S : TiO<sub>2</sub> = 3 : 7, with high degradation efficiency of almost 99% using methyl orange in 300 min and methylene blue in 180

min. This semiconductors association and the films homogeneity have the ability to limit the electron–hole recombination facilitating good efficiency in dyes photodegradation even under visible light irradiation. Huang *et al.*<sup>253</sup> prepared Cu<sub>2</sub>O nanoparticles and microparticles. They tested these particles for the photodegradation of methyl orange. It was observed that nanoparticles were stable in ambient atmosphere, whereas microparticles were found stable as a Cu<sub>2</sub>O/CuO core structure. The Cu<sub>2</sub>O microparticles with very slow photocorrosion rate exhibited a higher photocatalytic activity for methyl orange dye than that of the deactivated nanoparticles during the photocatalytic reaction.

**Sn<sup>4+</sup> doping.** Sn<sup>4+</sup> doped nanosized TiO<sub>2</sub> particles have several advantages compared to other TiO<sub>2</sub> powders. They have pure anatase crystalline form having high-dispersion ability both in polar or non-polar solvents. They also have fine particle size with more uniform distribution with stronger interfacial adsorption facilitating its easy coating on different supporting material.<sup>254</sup> The Sn<sup>4+</sup>-doped TiO<sub>2</sub> nanoparticles having molar doping ratio for Sn<sup>4+</sup> and tetrabutylorthotitanate of *ca.* 5 were synthesized by hydrothermal process at 225 °C. The double layers of these nanoparticles coated on glass surfaces were found to be having much higher photocatalytic performance under UV and Vis lights than pure TiO<sub>2</sub>.

### Noble metal modified TiO<sub>2</sub>

Deposition of noble metals on TiO<sub>2</sub> surface has been reported to improve the photocatalytic efficiency by acting as an electron trap due to the Schottky barrier formation thereby reducing electron–hole recombination process and helping interfacial charge transfer.<sup>79,255–261</sup> TiO<sub>2</sub> modified with noble metal exhibits excellent stability as well as high reproducibility. Doping of TiO<sub>2</sub> with noble metals for photo-oxidation has been studied for at least two decades. However, the detail about the most recent dye degradation work including Silver and Platinum doped TiO<sub>2</sub> is given below under separate headings.

**Silver modified TiO<sub>2</sub>.** Silver modified TiO<sub>2</sub> has shown promising results towards increased degradation efficiency and stability. Gupta *et al.*<sup>262</sup> were able to regenerate Ag<sup>+</sup> doped TiO<sub>2</sub> catalyst just by washing the catalyst thoroughly with distilled water. Photocatalytic activity of Ag<sup>+</sup> doped TiO<sub>2</sub> indicated >99% decolorization of basic violet 3 and methyl red within 90 min with a 86% mineralization efficiency. Seery *et al.*<sup>255</sup> reported an enhanced decolorization of rhodamine 6 G with Ag modified TiO<sub>2</sub> under visible light photocatalysis. Increase in decolorization is attributed to the increase in visible absorption capacity of silver nanoparticles. Whereas, Gunawan *et al.*<sup>263</sup> demonstrated the reversible photo-switching of nano silver on TiO<sub>2</sub>. Reduced silver on a TiO<sub>2</sub> support when exposed to visible light ( $\lambda > 450$  nm) resulted in electron excitation and its reverse flow to the TiO<sub>2</sub> support from silver by oxidizing silver ( $\text{Ag}^0 \rightarrow \text{Ag}^+$ ) in the process. For improved optical properties it would be more attractive to further tailor the band gap width of TiON/Ag<sub>2</sub>O with some potential transition metals.<sup>264</sup>

**Platinized TiO<sub>2</sub> nanoparticles.** Platinum deposited TiO<sub>2</sub> has been repeatedly used in a variety of photoreactions that speeds

up the water splitting reaction<sup>265,266</sup> and oxidation of organic compounds<sup>145,267,268</sup> and CO.<sup>269</sup> Platinum nanoparticles can be beneficial for the subsequent oxidative reaction steps in the presence of molecular oxygen, which allows direct oxidation of the organic compounds by holes and HO<sup>·</sup> radicals as well. The main effect of Pt-loaded TiO<sub>2</sub> is due to its higher production rate of oxidizing species, *e.g.* holes or HO<sup>·</sup> radicals than conventional heating operation.

### Multi-atom doped TiO<sub>2</sub>

Many studies have revealed that TiO<sub>2</sub> mono-doping may lead to recombination centers thereby inhibiting light-induced migration of charge carriers to the surface.<sup>270</sup> However, it has been recognized that co-doping of TiO<sub>2</sub> with both nonmetal and metal can reduce the number of recombination centers by neutralizing positive and negative charges inside the TiO<sub>2</sub>, which can effectively improve the efficiency of migration of the charge carriers and thus enhance photocatalytic activity.<sup>271</sup> Xing *et al.*<sup>272</sup> prepared carbon and lanthanum co-doped TiO<sub>2</sub> by a hydrothermal method and reported their high photocatalytic activity under both UV and visible-light irradiation. Recently, Yang *et al.*<sup>273</sup> synthesized Mo and C co-doped TiO<sub>2</sub> photocatalysts and reported that 1% Mo–C4/TiO<sub>2</sub> showed an excellent visible light photocatalytic degradation of rhodamine B dye. The prepared co-doped catalysts showed greater photocatalytic activity than pure anatase TiO<sub>2</sub> and the mono-doped catalysts, because a synergistic effect between molybdenum and carbon increases absorption of visible light and affects separation of photoinduced electrons and holes. Also, Yan *et al.*<sup>274</sup> investigated photocatalytic degradation of methyl orange by TiO<sub>2</sub>–SiO<sub>2</sub>–NiFe<sub>2</sub>O<sub>4</sub> suspensions and reported that OH radicals and h<sup>+</sup> plays important roles in the degradation by TiO<sub>2</sub>–SiO<sub>2</sub>–NiFe<sub>2</sub>O<sub>4</sub>. Akpan and Hameed<sup>275</sup> compared electronically stable composite photocatalyst of the type  $\text{Ti}^{(1-x-y)}\text{Ca}^{(3x-y)}\text{Ce}^{(2x-y)}\text{W}^{(y/6)}\text{O}_2^{(1-2(y-x))}$  (at  $y < 2x$  and  $x + y < 1$ ) prepared by sol-gel method with commercially available Degussa P-25 and TiO<sub>2</sub> photocatalysts for acid red 1 (AR1) photocatalytic degradation. The performance of the composite catalyst excelled that of TiO<sub>2</sub>, but was as good as Degussa P-25 in terms of the solar photodegradation. However, composite photocatalyst was found better than Degussa P-25 in terms of reusability since it could settle out of solution in less than one hour after solar experiment. The composite photocatalyst was found to have narrowed band gap as compared to TiO<sub>2</sub> by 0.26 eV with its activities more into visible region.

### Dye sensitization in photocatalysis

On a broader scale, waste water remediation with dye sensitization method is beneficial in two ways. *Firstly*, the adsorption of the dye on the surface of TiO<sub>2</sub> catalyst extends the absorption spectrum of TiO<sub>2</sub> from UV to visible regime.<sup>102</sup> *Secondly*, the system containing the dye and the phenolic compound represents a classic model of a real effluent stream, which is usually a mixture of different organic compounds, surfactants and metal ions. Dye sensitized degradation is primarily aided by enhanced adherence of the dye molecule onto TiO<sub>2</sub> surface in the presence

of  $O_2$  that can easily scavenge the injected electrons from the conduction band of  $TiO_2$ .<sup>76</sup> General mechanism of dye sensitized photocatalysis has been explained in detail in basic principles and mechanism section of this review. Zhang *et al.*<sup>276</sup> recently studied the aerobic selective oxidation of alcohols in the presence of an anthraquinonic dye (alizarin red S) sensitized  $TiO_2$ , and a nitroxyl radical (2,2,6,6-tetramethyl-piperidinyloxy). They found that the whole mechanism involved was the formation of a dye radical cation, which oxidized the nitroxyl radical. This oxidized radical species was found to be mainly responsible for the selective oxidation of alcohols into aldehydes. Other conjugated polymers such as poly(aniline)<sup>277</sup> and poly(thiophene)<sup>278</sup> has also been used as  $TiO_2$  sensitizers for the degradation of dyes.

Recently, there have been new discoveries related to the adsorption of complexants on  $TiO_2$  surface leading to a sharp enhancement in its activity under visible light by using absorbent such as salicylic acid.<sup>279</sup> In a study, Moser *et al.*<sup>280</sup> proved that surface complexation of colloidal semiconductors strongly enhance interfacial electron transfer rates. Ikeda *et al.*<sup>281</sup> demonstrated that phenolic compounds with  $TiO_2$  can work as catalyst under visible light below *ca.* 550–600 nm for water reduction in the presence of a sacrificial donor. Also, Zhang *et al.*<sup>282</sup> chemically modified  $TiO_2$  nanoparticles with catechol (4.0 wt% catechol/ $TiO_2$ ) without changing the crystalline structure of  $TiO_2$ . Surface complexation of catechol lead to an enhanced acid orange 7 dye photocatalytic degradation by shifting onset wavelength of the optical absorption to the visible range.

### Structurally modified $TiO_2$

For enhancement of photocatalysis, nanostructured materials with different shapes of  $TiO_2$  including nanoparticles, nanotubes, nanofibers, nanocages, nanorods, nanorings, nanosheets, nanocombs, nanobowls, nanosprings and nanobelts have been employed.<sup>283</sup> The discussion below illustrates the use of most common  $TiO_2$  structural modification to enhance its photocatalytic activity.  $TiO_2$  can be synthesized in the form a nanometer scale tube like structure called  $TiO_2$  nanotubes.<sup>284</sup> The photoactivity of the  $TiO_2$  nanotube films has been found as strongly influenced by the tube diameter and thickness.<sup>285,286</sup> Increasing tube thickness increases the photodegradation efficiency till a maximum and then decreases till a steady value. In much longer tubes active species have a longer diffusion path that may cause the decrease in photocatalytic degradation rate. The nanotube arrays have been found to be more active than anatase or P-25  $TiO_2$  nanoparticulate films with similar thickness and geometric area. The enhanced dye degradation activity is attributed to a more effective separation of electron–hole pairs taking place in a well ordered way in  $TiO_2$  nanotube array film and due to higher internal surface area of the nanotube structure.<sup>285–290</sup>

### Graphene modified $TiO_2$

Carbon can also be used in the form of graphene to synthesize graphene/ $TiO_2$  photocatalysts.<sup>291</sup> Graphene is an atomic sheet of  $sp^2$ -bonded carbon atoms with unique properties having high

conductivity, large specific surface area and high transparency due to its one-atom thickness.<sup>292</sup> Zhang *et al.*<sup>293</sup> prepared a P-25–graphene composite by hydrothermal treatment of a suspension of P-25 and graphene oxide. Graphene oxide was reduced to graphene and then P-25 nanoparticles were deposited simultaneously on this graphene sheet. The P-25–graphene composite was found more active than P-25 for the photodegradation of methylene blue due to reduced charge recombination and enhanced absorptivity. The P-25–graphene composite exhibited higher efficiency than P-25 having same carbon content, due to its giant two-dimensional planar structure, which facilitated a better platform for the adsorption of the dye and charge transportation.<sup>283</sup> Moreover,  $TiO_2$ /graphene composites have been well studied as a solar light photocatalysts and electrode materials for lithium-ion batteries. Recent reports have shown that ultralight 3D-graphene aerogels (GAs) can better adsorb organic pollutants and can provide multidimensional electron transport pathways. Qiu *et al.*<sup>294</sup> prepared 3D-structured  $TiO_2$ /GA composites by one-step hydrothermal method using glucose. Glucose acts as facet-controlling agent to achieve *in situ* growth of  $TiO_2$  nanocrystals on GAs surfaces.  $TiO_2$  nanocrystals exposed with {001} facets and mesoporous structure were highly dispersed on the GAs surface. Affording high surface area, massive appearance, and hydrophobic properties determine its high recyclability and to efficiently photodegrade methyl orange dye.

### Fullerenes modified $TiO_2$

A fullerene is anymolecule composed entirely of carbon, in the form of a hollow sphere, ellipsoid, tube, and many other shapes. Spherical fullerenes are also called buckyballs. Cylindrical fullerenes are called carbon nanotubes or buckytubes. Fullerenes are similar in structure to graphite, which is composed of stacked graphene sheets of linked hexagonal rings; but they may also contain pentagonal or sometimes heptagonal rings. Fullerenes are extremely hydrophobic, therefore, their use in aqueous media is quite limited. However functionalizing the molecules with hydroxyl groups can improve water solubilizing properties of fullerenes.<sup>283</sup> Krishna *et al.*<sup>295</sup> employed poly-hydroxy fullerenes (PHF) to enhance the photocatalytic efficiency of  $TiO_2$  for the degradation of the procion red dye. The PHF molecules adsorbed on the surface of  $TiO_2$  by electrostatic forces enabled the scavenging of the photogenerated electrons decreasing the electron/hole recombination. The surface coverage of the  $TiO_2$  nanoparticles by the PHF molecules ( $C_{60}(OH)_n$ ,  $n = 18–24$ ) determined the extent of enhancement in dye degradation, with an optimum PHF/ $TiO_2$  weight ratio equal to 0.001.<sup>296,297</sup>

### Improvement by enhancing $TiO_2$ reactive facets

For anatase  $TiO_2$ , theoretical and experimental studies have so far revealed that {001} facet compared to thermodynamically stable {101} facet is much more reactive being the dominant source of active sites for various applications.<sup>298</sup> Whereas, most of the synthetic anatase crystals due to its crystal growing process are dominated by the less-reactive {101} facets

diminishing the reactive {001} facets to minimize the surface energy. Chen *et al.*<sup>299</sup> presented a simple hydrothermal approach for synthesizing uniform, hierarchical spheres self-organized from ultrathin anatase  $\text{TiO}_2$  nanosheets with nearly 100% exposed {001} facets. Also, Liu *et al.*<sup>300</sup> reported fabricating hollow  $\text{TiO}_2$  microspheres composed of anatase polyhedra with 20% exposed {001} facets by fluoride-mediated self-transformation method, exhibiting tunable photocatalytic selectivity in decomposing azo dyes in water. Very recently, Yu *et al.*<sup>301</sup> synthesized of layered  $\text{TiO}_2$ , composed of nanosheets with exposed {001} facets, by a simple hydrothermal method. It was observed that layered  $\text{TiO}_2$  with {001} facet nanosheets exhibited excellent photocatalytic activity for the degradation of rhodamine B dye.

## Practical aspects of $\text{TiO}_2$ photo-processes

### Limitations of $\text{TiO}_2$ photo-processes

Performance of a catalyst depends upon its configurations *i.e.* suspended or fixed-bed catalyst impart different performances. Although, coating a catalyst eliminates the need for its post-filtration and centrifugation but it generally reduces the system efficiency significantly largely due to loss in exposed surface area.<sup>302,303</sup> On the other hand disadvantages using powder form of catalyst include stirring during the reaction and separation of catalyst from the treated water after each run. To address the later, filtration, sedimentation and centrifugation processes have been used to recover highly dispersed and suspended catalyst from the treated water. However, with this method a fraction of  $\text{TiO}_2$  particles usually remains in the treated water and a further microfiltration step is usually required for final purification. Besides its time consuming problem, the filtration process become increasingly inefficient as the particle size diminishes. Smaller particles suspended in the water may penetrate through filtration materials causing membranes filter clogging.<sup>304</sup>

The other common way to perform the separation is by sedimentation of  $\text{TiO}_2$  particles after pH adjustment by coagulation-flocculation process. Separation by sedimentation has been enhanced by attaching  $\text{TiO}_2$  particles onto other support particles like quartz, silica gel, alumina, zeolites, activated carbon or glass spheres but the loss of photocatalytic activity has usually been observed.<sup>305</sup> In addition to this the fast aggregation of  $\text{TiO}_2$  in suspension leads to a decrease in effective surface area which reduces its catalytic efficiency. A filtration step after photocatalytic reaction is still required because of  $\text{TiO}_2$  suspension.<sup>164</sup> Moreover,  $\text{TiO}_2$  absorption wavelength corresponding to the band-gap energy of 3.02 eV is at near ultraviolet radiation.<sup>306</sup> Thus either the need of an UV excitation source or ability of  $\text{TiO}_2$  to absorb only 5% energy of the solar spectrum has restricted its technological applications.

### Trends in improving $\text{TiO}_2$ photo-processes

Despite of drawbacks discussed in the above section, more coated photocatalysts and immobilization techniques are still

been investigated.<sup>164,307-311</sup> In many cases  $\text{TiO}_2$  coated on a support is found to be more efficient for organic compound removal in contrast to uncoated  $\text{TiO}_2$ , reducing overall operating costs.<sup>312</sup> Many researchers have examined some methods for fixing  $\text{TiO}_2$  on supporting materials including glass beads,<sup>313</sup> fiber glass,<sup>161,314</sup> activated carbon,<sup>315</sup> silica<sup>316</sup> and zeolite<sup>317</sup> as given in Table 3.

### Zeolite as $\text{TiO}_2$ support

Zeolites are the aluminosilicate members of the family of microporous solids known as molecular sieves. The term molecular sieve refers to the ability to selectively sort molecules based primarily on a size exclusion process. This is due to a very regular pore structure of molecular dimensions. Among variety of supports available, zeolites are considered to provide an effective electric field of their framework for separation of photogenerated electrons and holes.<sup>318,324</sup> However care should be taken while using zeolite as  $\text{TiO}_2$  support so that it may not affect the  $\text{TiO}_2$  photoactivity and the adsorptive properties of zeolite. Mathews<sup>325</sup> reported that photoefficiency of  $\text{TiO}_2$  is suppressed when Ti interacts with zeolite. The OH available on the surface of  $\text{TiO}_2$  can be easily transferred onto zeolite surface as shown in Fig. 8. Additionally, the presence of zeolite on  $\text{TiO}_2$  maintains dye molecules near the photocatalyst (local concentration effect) which may result in an increase of degradation rate.

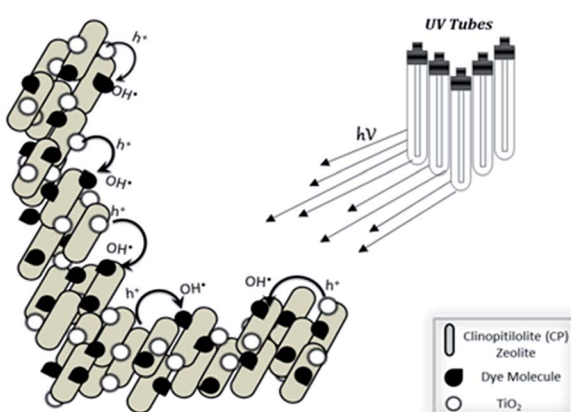
### $\text{TiO}_2$ loaded hydrophobic mesocellular foams

Hydrophobic materials based on zeolites and mesoporous silicas such as hexagonal mesoporous silica (HMS), SBA-15 and mesocellular foams could offer excellent ability of adsorption of organic compounds owing to their weak adsorption of water molecules and the large surface areas.<sup>326</sup> Though simple surface fluorination on  $\text{TiO}_2$  can induce an enhanced UV light photocatalytic oxidation activity, however it is difficult to improve the visible light photocatalytic activity of  $\text{TiO}_2$ , owing to the lack of photo-excited holes in the visible light irradiation.<sup>327</sup>

In 2012, Xing *et al.*<sup>328</sup> prepared a novel hydrophobic  $\text{TiO}_2$  photocatalyst, which can enhance visible light response by using cheaper and low-toxic inorganic  $\text{NH}_4\text{F}$ . They prepare the super-hydrophobic mesocellular foams loaded with nanosized  $\text{TiO}_2$  photocatalyst. Mesoporous catalyst greatly facilitated the surface fluorination, which together with  $\text{Ti}^{3+}$  (a self-doped  $\text{TiO}_2$  catalyst) generation promoted its visible light photocatalytic activity<sup>329</sup> and the surface fluorination enhanced UV light photocatalytic activity. It was reported that the catalyst exhibit permanent and excellent super-hydrophobic property, high adsorption capacity, and enhanced photocatalytic activity for rhodamine B (RhB) degradation. Recently, Qi *et al.*<sup>330</sup> prepared carbon-doped  $\text{TiO}_2$ /mesocellular-F photocatalysts hydrophobically modified by the hydrothermal method. Catalyst indicated an efficient visible light photodegradation of methyl orange solution because of the synergistic effect of small crystal size, carbon dopants, and hydrophobic modification due to the fluorination of  $\text{NH}_4\text{F}$ .

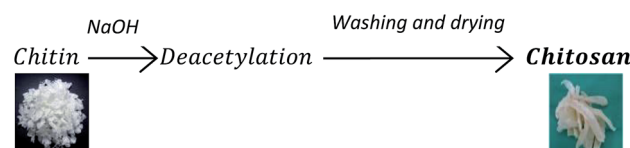
Table 3 Types of the supports used for enhancing  $\text{TiO}_2$  photocatalytic degradation of different dyes

Support type	Dye used for degradation	Technique used for preparation	Performance	Ref.
Clinoptilolite (CP) (Iranian Natural Zeolite)	Acid red 114	—	$\text{TiO}_2/\text{clinoptilolite}$ (SSD) proved to be an active photocatalyst with a first order reaction, $k = 0.0108 \text{ min}^{-1}$ . With increasing dye conc. photodegradation conversion of AR 114 decreased	318
Chitosan [ $\beta$ -(1 $\rightarrow$ 4)-2-amino-2-deoxy- $\alpha$ -D-glucose]	Methyl orange	Solution casting technology	The $\text{TiO}_2/\text{ZnO}/\text{chitosan}$ NTFs showed high photocatalytic activity under solar irradiation	319
Polymethylmethacrylate (PMMA) rings	Methylene blue	Ultrasonically spray-coated with $\text{TiO}_2$ sol	Results showed 80% degradation of methylene blue after 10 min at pH 9	320
Polyamide 6 (PA6) fiber	Methylene blue	Low temperature hydrothermal method	Compared with the untreated fabric, the protection against UV radiation improved. The titanium dioxide coated fabric could degrade methylene blue efficiently dye under UV irradiation	321
Glass plates	Acid red 27 (AR27)	Immobilized	Outlet stream from photoreactor was mineralized with products such as $\text{NH}_4^+$ , $\text{NO}_3^-$ , $\text{O}_2^-$ and $\text{SO}_4^{2-}$ ions	322
Non-woven paper with $\text{SiO}_2$	Reactive black 5 (RB5)	—	Degradation of RB5 azo dye was strongly influenced by the ionic strength of the solution. Above pH PZC of $\text{SiO}_2$ , the cations of the solution increased the amount of dye adsorbed onto the photocatalyst support	170
Sand	Methylene blue, rhodamine B and methyl orange	—	$\text{TiO}_2/\text{UV}$ process supported on sand is effective in totally mineralizing these compounds	323

Fig. 8 Synergistic effect of  $\text{TiO}_2$  and clinoptilolite catalyst on dye degradation by producing  $\text{OH}^-$  free radicals.<sup>318</sup>

### Chitosan as $\text{TiO}_2$ support

Chitosan [ $\beta$ -(1  $\rightarrow$  4)-2-amino-2-deoxy- $\alpha$ -D-glucose] is a natural cationic biopolymer that is produced by *N*-deacetylation of chitin. Chitin is considered as the second most abundant natural polysaccharide after cellulose.<sup>331</sup> The extraction of chitin from shells and its subsequent deacetylation to chitosan is a relatively low cost process.<sup>332</sup>



Chitosan molecules contain a large number of reactive hydroxyl ( $-\text{OH}$ ) and amino ( $-\text{NH}_2$ ) groups. Also, chitosan has

high affinity for metal ions and this property has been used to prepare metal–chitosan nanocomposites.<sup>333</sup> This enables Chitosan to exhibit unique adsorption and chelating properties for all kinds of heavy metal ions,<sup>334–336</sup> making chitosan an appropriate and excellent bio-matrix for synthesizing nanosized particles for various inorganic photocatalysts such as titanium oxide,<sup>337,338</sup> cadmium sulfide,<sup>319,339</sup> zinc sulfide,<sup>340</sup> zinc oxide<sup>341</sup> and cuprous oxide.<sup>342</sup> In addition, immobilizing nanosized photocatalysts onto chitosan bio-matrix can effectively prevent agglomeration of nanoparticles during growth and can overcome the difficulties related to separation and recovery of nanosized powder materials.<sup>336</sup>

### Activated carbon as $\text{TiO}_2$ support

Activated carbon also known as activated charcoal (AC) is a highly porous form of carbon with porosity spanning the macro ( $\lambda > 50$  nm), meso (0.5–1  $\mu\text{m}$ ) and micro ( $< 1 \mu\text{m}$ ) pore ranges<sup>116</sup> and very high-surface typically up to 900–1200  $\text{m}^2 \text{ g}^{-1}$ .<sup>343</sup> It is generally produced from cheap carbonaceous source materials such as nutshells, coconut husk, peat, wood, coir, lignite, coal, and petroleum pitch. Use of activated carbon is the most common method applied for dye removal by adsorption.<sup>344</sup> In particular, activated carbon (AC) has been extensively researched as a support for heterogeneous catalysis,<sup>345</sup> and there exists over 650 studies and well over 1000 patents<sup>346</sup> concerning AC– $\text{TiO}_2$  mixtures or composites.<sup>347–351</sup> Due to its higher effectiveness, it has been applied on adsorbing cationic, mordant, and acid dyes and to dispersed, vat, direct, pigment and reactive dyes on a slightly lesser extent.<sup>26,352</sup>

Effective performance using activated carbon mainly dependents upon the type of carbon being used and the characteristics of the aqueous solution containing various chemicals and non-targeted contaminants. Regeneration or reuse can result in a steep reduction in performance, and efficiency of dye removal. Activated carbon, like many other dye-removal treatments is considered suitable for one particular type of pollutant or waste system and ineffective on another. Although, activated carbon is expensive it comes with the advantage of regeneration. However, this reactivation usually results into 10–15% loss of the sorbent. Arana *et al.*<sup>353</sup> prepared AC and  $\text{TiO}_2$  catalysts having varying proportion. The results showed that the AC in addition to increasing surface area can also modify the acid–base properties and the UV spectrum of  $\text{TiO}_2$ . It was reported that activity of AC was increased under solar irradiation.

In AC– $\text{TiO}_2$  system, the adsorption capacity of AC enhances the chances of high concentration of reactants to come in contact with  $\text{TiO}_2$  and possibly turning them into their intermediates as explained in the Fig. 9. Zhang *et al.*<sup>236</sup> proposed a similar illustration for the photocatalyzed mineralization of methyl orange to understand the effect of presence of AC onto  $\text{TiO}_2$  for effective dye degradation. On the other hand, a disadvantage of using AC is the excessive formation of nanosized pores resulting into rare infiltration, leaving  $\text{TiO}_2$  on the outer macropores.<sup>116,354,355</sup> Moreover, the band gap tuning problem of  $\text{TiO}_2$  is not resolved by the use of AC as a support.

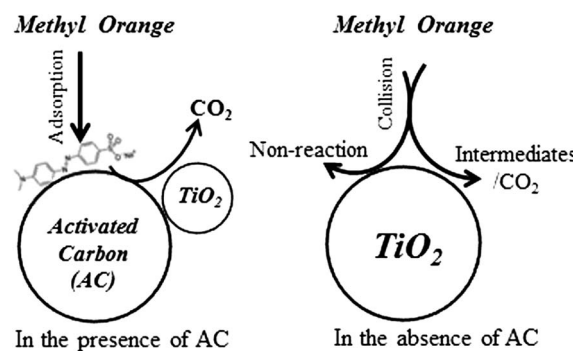


Fig. 9 Synergistic mechanism between AC– $\text{TiO}_2$  composites. The arrow labelling un-reacted emphasizes that in the absence of Absorbent the reactants may remain un-reacted into the solution resulting in low photoactivity of methyl orange.<sup>236</sup>

### Silica as $\text{TiO}_2$ support

Use of supported  $\text{TiO}_2$  catalysts depends on the nature of supports, one of the most important factors influencing photocatalytic performance.<sup>169,356,357</sup> Recently, amorphous  $\text{SiO}_2$  due to its special physicochemical properties such as high adsorption capacity has been studied showing advantages towards highly active support for catalysts. The presence of considerably large number of acid sites and hydroxyl groups on the surface of amorphous  $\text{SiO}_2$  material make it more absorptive.<sup>358,359</sup> Studies have shown that silica gel can be an effective support for binding  $\text{TiO}_2$  that is effective for removal of basic dyes. However, in such processes, there can be side reaction taking place along with photocatalysis and therefore such limiting factors can prevent its commercial application.<sup>26</sup> Additionally, immobilization  $\text{TiO}_2$  on a suitable and inert matrix has shown an advanced organic and inorganic pollutant photodecomposition than that of pure  $\text{TiO}_2$ .<sup>169,360</sup>

Sun *et al.*<sup>361</sup> investigated the catalytic properties of three porous amorphous silica including diatomite, opal and porous supported photocatalysts ( $\text{TiO}_2/\text{SiO}_2$ ) by UV-assisted degradation of rhodamine B. Through morphology and physical properties of the resulting  $\text{TiO}_2$ /amorphous  $\text{SiO}_2$  catalysts, it was suggested that the nature of silica supports could affect the particle size and the crystal form of  $\text{TiO}_2$ .  $\text{TiO}_2$ /diatomite photocatalyst, compared with pure  $\text{TiO}_2$  (P-25) and the other two  $\text{TiO}_2$ /amorphous  $\text{SiO}_2$  catalysts, exhibited better catalytic performance at different calcination temperatures with a discolouration rate of up to over 85%. Photocatalytic properties such as mixed-phase  $\text{TiO}_2$  with small particle size might be responsible for efficient performance. Furthermore, its stable and inert porous structure improves its activity.

### Carbon nanotubes as $\text{TiO}_2$ support

The carbon nanotubes (CNTs) are interesting materials having unique electronic properties associated with their special 1D structure which facilitates the charge transfer.<sup>362</sup> The CNTs are described as tubular assemblies made exclusively of rolled-up films of interlocked carbon atoms. These are classified as single-walled carbon nanotubes (SWCNTs) which consist of a

single layer of graphene sheet rolled into a cylindrical tube or multi-walled carbon nanotubes (MWCNTs), which contain multiple concentric tubes. CNTs have a large specific surface area due to their hollow geometry. CNTs-TiO<sub>2</sub> hybrids have been tested for the photodegradation of acetone,<sup>363</sup> methylene blue<sup>364,365</sup> and phenol.<sup>366,367</sup> All such studies emphasized that the addition of CNTs had enhanced the photocatalytic effectiveness of TiO<sub>2</sub>.

Yu *et al.*<sup>368</sup> compared the effect of MWCNTs on the adsorption and the photocatalytic properties of TiO<sub>2</sub> P-25. The results showed that the mixture of CNTs and TiO<sub>2</sub> significantly improved the photocatalytic activity of TiO<sub>2</sub> for the treatment of three azo dyes and was found more efficient than the mixture of TiO<sub>2</sub> with activated carbon. Luo *et al.*<sup>369</sup> prepared short MWCNTs that can be suspended, sorted and manipulated more easily so that the light can well penetrate into the inner tubes. The short MWCNTs were used as initial materials to fabricate TiO<sub>2</sub>/short MWCNTs nano-composites that were tested for the photodegradation of reactive brilliant red X-3B. The photoactivity of the TiO<sub>2</sub>/short MWCNTs samples with optimum weight ratio (1 : 100) was studied and rates much higher than that of various active photocatalysts (TiO<sub>2</sub>/short MWCNTs > TiO<sub>2</sub>/MWCNTs > TiO<sub>2</sub>> P-25) were reported.

### TiO<sub>2</sub> embedded in polymer matrix

Difficulties such as low quantum yield and low adsorption capacity of TiO<sub>2</sub> photocatalyst limits its practical application.<sup>122</sup> Among multiple techniques to overcome these issues, incorporation of semiconductors into the polymer matrix have been achieved. Example such as polypyrrole (PPy)-TiO<sub>2</sub> composite films, polyethylene-TiO<sub>2</sub>, and polyvinylchloride (PVC)-TiO<sub>2</sub> as resulting composites were found to enhance degradation reactions more effectively than a suspension of TiO<sub>2</sub> nanoparticles.<sup>370</sup> Cheng *et al.*<sup>371</sup> report efficient adsorption and photodegradation of textile dyes orange II and methyl orange under UV irradiation using polyaniline (PANI) and PANI-TiO<sub>2</sub> composite nanotubes as photocatalyst, respectively. Decolorization up to 98.6% of orange II and 98.1% of methyl orange in the presence of PANI-TiO<sub>2</sub> composite nanotubes were reported. Addition of TiO<sub>2</sub> nanoparticles to the one-dimensional polymer matrix gradually increased the removal rate of organic dyes due to higher specific surface area and the positive form of titania at the interface.

## Conclusion

Owing to its many advantages mainly involving most stable and active naturally occurring photocatalyst, TiO<sub>2</sub> is, so far, seen as the best catalytic material for degradation of various contaminants and sustainable environmental remediation technology. It has been widely employed in dye photodegradation studies. Photodegradation of industrial dyes using improved TiO<sub>2</sub> has presented a somewhat promising and effective treatment technology. However, in order to overcome constraint such as sensitivity towards operational parameters *i.e.* pH, temperature, catalyst dose, amount of dye, inability for high photon efficiency

to utilize wider solar spectra, and separation after treatment inhibits the ability of TiO<sub>2</sub> from its real time application on a vast scale. Therefore, more advanced level research studies are needed to address TiO<sub>2</sub> shortfalls or to formulate potential alternative for TiO<sub>2</sub>.

## Acknowledgements

The authors of this work acknowledge the financial support from Department of Environmental Sciences, Quaid-i-Azam University, Islamabad and Higher Education Commission of Pakistan.

## Notes and references

- 1 R. J. Fessenden and J. S. Fessenden, *Adv. Drug Res.*, 1967, **4**, 95–132.
- 2 H. Park and W. Choi, *J. Photochem. Photobiol. A*, 2003, **159**, 241–247.
- 3 I. A. Alaton, I. A. Balcioglu and D. W. Bahnemann, *Water Res.*, 2002, **36**, 1143–1154.
- 4 U. Pagga and D. Brown, *Chemosphere*, 1986, **15**, 479–491.
- 5 N. Bensalah, M. Alfaro and C. Martínez-Huitle, *Chem. Eng. J.*, 2009, **149**, 348–352.
- 6 K. Turhan and Z. Turgut, *Desalination*, 2009, **242**, 256–263.
- 7 F. Gosetti, V. Gianotti, S. Angioi, S. Polati, E. Marengo and M. C. Gennaro, *J. Chromatogr. A*, 2004, **1054**, 379–387.
- 8 A. Houas, H. Lachheb, M. Ksibi, E. Elaloui, C. Guillard and J.-M. Herrmann, *Appl. Catal. B*, 2001, **31**, 145–157.
- 9 H. Zollinger, *Color chemistry: syntheses, properties, and applications of organic dyes and pigments*, Wiley-VCH, 2003.
- 10 W. S. Perkins, *Textile Chemist and Colorist and American Dyestuff Reporter*, 1999, vol. 1, pp. 33–37.
- 11 I. K. Konstantinou and T. A. Albanis, *Appl. Catal. B*, 2004, **49**, 1–14.
- 12 R. Kant, *Nat. Sci.*, 2012, **04**, 22–26.
- 13 R. Anliker, *Ecotoxicol. Environ. Saf.*, 1979, **3**, 59–74.
- 14 J. Shore, *Indian Journal of Fiber and Textile Research*, 1996, **21**, 1–29.
- 15 C. Carliell, S. Barclay and C. Buckley, *Water SA*, 1996, **22**, 225–233.
- 16 N. Willmott, J. Guthrie and G. Nelson, *J. Soc. Dyers Colour.*, 1998, **114**, 38–41.
- 17 G. Mishra and M. Tripathy, *Colourage*, 1993, **40**, 35.
- 18 M. Senthilkumar and M. Muthukumar, *Dyes Pigm.*, 2007, **72**, 251–255.
- 19 R. Leena and S. Raj, *Afr. J. Biotechnol.*, 2008, **71**(8), 3309–3313.
- 20 G. L. Baughman and T. A. Perenich, *Environ. Toxicol. Chem.*, 1988, **7**, 183–199.
- 21 K.-T. Chung, G. E. Fulk and M. Egan, *Appl. Environ. Microbiol.*, 1978, **35**, 558–562.
- 22 E. J. Weber and R. L. Adams, *Environ. Sci. Technol.*, 1995, **29**, 1163–1170.
- 23 U. Bali, E. Catalkaya and F. Sengul, *J. Hazard. Mater.*, 2004, **114**, 159–166.
- 24 M. Rauf and S. S. Ashraf, *Chem. Eng. J.*, 2009, **151**, 10–18.

25 N. Daneshvar, M. Rasoulifard, A. Khataee and F. Hosseinzadeh, *J. Hazard. Mater.*, 2007, **143**, 95–101.

26 T. Robinson, G. McMullan, R. Marchant and P. Nigam, *Bioresour. Technol.*, 2001, **77**, 247–255.

27 A. G. Prado, L. B. Bolzon, C. P. Pedroso, A. O. Moura and L. L. Costa, *Appl. Catal., B*, 2008, **82**, 219–224.

28 A. Cassano, R. Molinari, M. Romano and E. Drioli, *J. Membr. Sci.*, 2001, **181**, 111–126.

29 G. Crini, *Bioresour. Technol.*, 2006, **97**, 1061–1085.

30 M. Perez-Urquiza and J. Beltran, *J. Chromatogr. A*, 2000, **898**, 271–275.

31 F. Hueber-Becker, G. J. Nohynek, E. K. Dufour, W. J. Meuling, A. T. H. de Bie, H. Toutain and H. M. Bolt, *Food Chem. Toxicol.*, 2007, **45**, 160–169.

32 D. Wróbel, A. Boguta and R. M. Ion, *J. Photochem. Photobiol., A*, 2001, **138**, 7–22.

33 L. Yang, Y. Lin, J. Jia, X. Xiao, X. Li and X. Zhou, *J. Power Sources*, 2008, **182**, 370–376.

34 N. I. Georgiev, V. B. Bojinov and P. S. Nikolov, *Dyes Pigm.*, 2009, **81**, 18–26.

35 R. Nilsson, R. Nordlinder, U. Wass, B. Meding and L. Belin, *Br. J. Ind. Med.*, 1993, **50**, 65–70.

36 W. Walthall and J. Stark, *Environ. Pollut.*, 1999, **104**, 207–215.

37 S. Tsuda, M. Murakami, N. Matsusaka, K. Kano, K. Taniguchi and Y. F. Sasaki, *Toxicol. Sci.*, 2001, **61**, 92–99.

38 C. Zaharia and D. Suteu, Adsorption of cationic dye on cellolignin, *BioResources*, 2012, **8**(1), 427–446.

39 A. Price, A. C. Cohen and I. Johnson, *J.J. Pizzuto's fabric science*, Fairchild Publications, New York, 8th edn, 2005.

40 R. M. Christie, *Colour chemistry*, Royal Society of Chemistry, 2001.

41 B. P. Corbman and M. D. Potter, *Textiles: Fiber to Fabric*, McGraw-Hill New York, NY, USA, 1975.

42 A. Datyner, *Rev. Prog. Color. Relat. Top.*, 1993, **23**, 40–50.

43 C. Stead, *Dyes Pigm.*, 1982, **3**, 161–171.

44 V. Golob and A. Ojstršek, *Dyes Pigm.*, 2005, **64**, 57–61.

45 P. E. McGovern and R. H. Michel, *Acc. Chem. Res.*, 1990, **23**, 152–158.

46 H. L. Needles, *Handbook of textile fibers, dyes and finishes*, Garland STPM Press, 1981.

47 W. Z. Tang and A. Huren, *Chemosphere*, 1995, **31**, 4157–4170.

48 M. A. Brown and S. C. De Vito, *Crit. Rev. Environ. Sci. Technol.*, 1993, **23**, 249–324.

49 Y. M. Slokar and A. Majcen Le Marechal, *Dyes Pigm.*, 1998, **37**, 335–356.

50 M. Sleiman, D. Vildozo, C. Ferronato and J.-M. Chovelon, *Appl. Catal., B*, 2007, **77**, 1–11.

51 W. Kuo, *Water Res.*, 1992, **26**, 881–886.

52 N. Ince and D. Gönenç, *Environ. Technol.*, 1997, **18**, 179–185.

53 O. Tünay, I. Kabdasli, G. Eremektar and D. Orhon, *Water Sci. Technol.*, 1996, **34**, 9–16.

54 M. Saquib and M. Muneer, *Dyes Pigm.*, 2003, **56**, 37–49.

55 E. P. Reddy, L. Davydov and P. Smirniotis, *Appl. Catal., B*, 2003, **42**, 1–11.

56 O. J. Hao, H. Kim and P.-C. Chiang, *Crit. Rev. Environ. Sci. Technol.*, 2000, **30**, 449–505.

57 A. Moutaouakkil, Y. Zeroual, F. Zohra Dzayri, M. Talbi, K. Lee and M. Blaghen, *Arch. Biochem. Biophys.*, 2003, **413**, 139–146.

58 C. Shaw, C. Carliell and A. Wheatley, *Water Res.*, 2002, **36**, 1993–2001.

59 G. M. Bonser, L. Bradshaw, D. Clayson and J. Jull, *Br. J. Cancer*, 1956, **10**, 539.

60 I. Arslan and I. A. Balcioğlu, *Dyes Pigm.*, 1999, **43**, 95–108.

61 K. Kunitou, S. Maeda, S. Hongyou and K. Mishima, *Can. J. Chem. Eng.*, 2002, **80**, 208–213.

62 S. Chakrabarti and B. K. Dutta, *J. Hazard. Mater.*, 2004, **112**, 269–278.

63 J. Sun, X. Wang, J. Sun, R. Sun, S. Sun and L. Qiao, *J. Mol. Catal. A: Chem.*, 2006, **260**, 241–246.

64 J. Madhavan, P. Maruthamuthu, S. Murugesan and S. Anandan, *Appl. Catal., B*, 2008, **83**, 8–14.

65 X.-H. Qi, Y.-Y. Zhuang, Y.-C. Yuan and W.-X. Gu, *J. Hazard. Mater.*, 2002, **90**, 51–62.

66 P. Pizarro, C. Guillard, N. Perol and J.-M. Herrmann, *Catal. Today*, 2005, **101**, 211–218.

67 H. Yates, M. Nolan, D. Sheel and M. Pemble, *J. Photochem. Photobiol., A*, 2006, **179**, 213–223.

68 M. Ni, M. K. Leung, D. Y. Leung and K. Sumathy, *Renewable Sustainable Energy Rev.*, 2007, **11**, 401–425.

69 L.-C. Chen and T.-C. Chou, *Ind. Eng. Chem. Res.*, 1994, **33**, 1436–1443.

70 G. Annadurai, T. Sivakumar and S. R. Babu, *Bioprocess Eng.*, 2000, **23**, 167–173.

71 W. A. Sadik, A. W. Nashed and A.-G. M. El-Demerdash, *J. Photochem. Photobiol., A*, 2007, **189**, 135–140.

72 Y. Jiang, Y. Sun, H. Liu, F. Zhu and H. Yin, *Dyes Pigm.*, 2008, **78**, 77–83.

73 E. Bizani, K. Fytianos, I. Poulios and V. Tsiridis, *J. Hazard. Mater.*, 2006, **136**, 85–94.

74 K. Vinodgopal and P. V. Kamat, *Environ. Sci. Technol.*, 1995, **29**, 841–845.

75 C. Chen, X. Li, W. Ma, J. Zhao, H. Hidaka and N. Serpone, *J. Phys. Chem. B*, 2002, **106**, 318–324.

76 K. Vinodgopal, D. E. Wynkoop and P. V. Kamat, *Environ. Sci. Technol.*, 1996, **30**, 1660–1666.

77 U. G. Akpan and B. H. Hameed, *J. Hazard. Mater.*, 2009, **170**, 520–529.

78 W. Tang, Z. Zhang, H. An, M. Quintana and D. Torres, *Environ. Technol.*, 1997, **18**, 1–12.

79 X. Li and F. Li, *Environ. Sci. Technol.*, 2001, **35**, 2381–2387.

80 Y. Wang, *Water Res.*, 2000, **34**, 990–994.

81 M. Styliidi, D. I. Kondarides and X. E. Verykios, *Appl. Catal., B*, 2003, **40**, 271–286.

82 K. Tanaka, K. Padermpole and T. Hisanaga, *Water Res.*, 2000, **34**, 327–333.

83 H. Lachheb, E. Puzenat, A. Houas, M. Ksibi, E. Elaloui, C. Guillard and J.-M. Herrmann, *Appl. Catal., B*, 2002, **39**, 75–90.

84 C. A. K. Gouvêa, F. Wypych, S. G. Moraes, N. Durán, N. Nagata and P. Peralta-Zamora, *Chemosphere*, 2000, **40**, 433–440.

85 A. Bianco Prevot, C. Baiocchi, M. C. Brussino, E. Pramauro, P. Savarino, V. Augugliaro, G. Marcì and L. Palmisano, *Environ. Sci. Technol.*, 2001, **35**, 971–976.

86 F. Zhang, J. Zhao, T. Shen, H. Hidaka, E. Pelizzetti and N. Serpone, *Appl. Catal., B*, 1998, **15**, 147–156.

87 J. Zhao, T. Wu, K. Wu, K. Oikawa, H. Hidaka and N. Serpone, *Environ. Sci. Technol.*, 1998, **32**, 2394–2400.

88 J. T. Spadaro, L. Isabelle and V. Renganathan, *Environ. Sci. Technol.*, 1994, **28**, 1389–1393.

89 B. Neppolian, H. C. Choi, S. Sakthivel, B. Arabindoo and V. Murugesan, *Chemosphere*, 2002, **46**, 1173–1181.

90 S. Sakthivel, B. Neppolian, M. V. Shankar, B. Arabindoo, M. Palanichamy and V. Murugesan, *Sol. Energy Mater. Sol. Cells*, 2003, **77**, 65–82.

91 C. M. So, M. Y. Cheng, J. C. Yu and P. K. Wong, *Chemosphere*, 2002, **46**, 905–912.

92 C. Hu, J. C. Yu, Z. Hao and P. K. Wong, *Appl. Catal., B*, 2003, **42**, 47–55.

93 C. Minero, V. Maurino and E. Pelizzetti, *Res. Chem. Intermed.*, 1997, **23**, 291–310.

94 H. Chun and W. Yizhong, *Chemosphere*, 1999, **39**, 2107–2115.

95 V. Augugliaro, C. Baiocchi, A. Bianco Prevot, E. García-López, V. Loddo, S. Malato, G. Marcì, L. Palmisano, M. Pazzi and E. Pramauro, *Chemosphere*, 2002, **49**, 1223–1230.

96 K. Nohara, H. Hidaka, E. Pelizzetti and N. Serpone, *J. Photochem. Photobiol., A*, 1997, **102**, 265–272.

97 V. Maurino, C. Minero, E. Pelizzetti, P. Piccinini, N. Serpone and H. Hidaka, *J. Photochem. Photobiol., A*, 1997, **109**, 171–176.

98 M. Abdullah, G. K. C. Low and R. W. Matthews, *J. Phys. Chem.*, 1990, **94**, 6820–6825.

99 M. Kerzhentsev, C. Guillard, J.-M. Herrmann and P. Pichat, *Catal. Today*, 1996, **27**, 215–220.

100 K. Pirkanniemi and M. Sillanpää, *Chemosphere*, 2002, **48**, 1047–1060.

101 M. Styliidi, D. I. Kondarides and X. E. Verykios, *Appl. Catal., B*, 2004, **47**, 189–201.

102 S. Kaur and V. Singh, *J. Hazard. Mater.*, 2007, **141**, 230–236.

103 C. Kormann, D. Bahnemann and M. R. Hoffmann, *Environ. Sci. Technol.*, 1991, **25**, 494–500.

104 W. Liu, S. Chen, W. Zhao and S. Zhang, *Desalination*, 2009, **249**, 1288–1293.

105 J. M. Peralta-Hernández, Y. Meas-Vong, F. J. Rodríguez, T. W. Chapman, M. I. Maldonado and L. A. Godínez, *Water Res.*, 2006, **40**, 1754–1762.

106 S. Lakshmi, R. Renganathan and S. Fujita, *J. Photochem. Photobiol., A*, 1995, **88**, 163–167.

107 D. C. Hurum, A. G. Agrios, K. A. Gray, T. Rajh and M. C. Thurnauer, *J. Phys. Chem. B*, 2003, **107**, 4545–4549.

108 H. Yin, Y. Wada, T. Kitamura, S. Kambe, S. Murasawa, H. Mori, T. Sakata and S. Yanagida, *J. Mater. Chem.*, 2001, **11**, 1694–1703.

109 A. Riga, K. Soutsas, K. Ntampagliotis, V. Karayannis and G. Papapolymerou, *Desalination*, 2007, **211**, 72–86.

110 V. K. Gupta, R. Jain, A. Nayak, S. Agarwal and M. Shrivastava, *Mater. Sci. Eng., C*, 2011, **31**, 1062–1067.

111 M. A. Nadeem, K. A. Connelly and H. Idriss, *Int. J. Nanotechnol.*, 2012, **9**, 121–162.

112 A. Shiga, A. Tsujiko, S. Yae and Y. Nakato, *Bull. Chem. Soc. Jpn.*, 1998, **71**, 2119–2125.

113 G. Riegel and J. R. Bolton, *J. Phys. Chem.*, 1995, **99**, 4215–4224.

114 M. Abdullah, G. K. Low and R. W. Matthews, *J. Phys. Chem.*, 1990, **94**, 6820–6825.

115 Z. Zhang, W. Wang, M. Shang and W. Yin, *J. Hazard. Mater.*, 2010, **177**, 1013–1018.

116 L. F. Velasco, J. B. Parra and C. O. Ania, *Appl. Surf. Sci.*, 2010, **256**, 5254–5258.

117 A. Khataee, M. Fathinia, S. Aber and M. Zarei, *J. Hazard. Mater.*, 2010, **181**, 886–897.

118 S. Sreekantan and L. C. Wei, *J. Alloys Compd.*, 2010, **490**, 436–442.

119 H.-F. Yu and S.-T. Yang, *J. Alloys Compd.*, 2010, **492**, 695–700.

120 K. Naeem and F. Ouyang, *Phys. B*, 2010, **405**, 221–226.

121 M. A. Fox and M. T. Dulay, *Chem. Rev.*, 1993, **93**, 341–357.

122 M. R. Hoffmann, S. T. Martin, W. Choi and D. W. Bahnemann, *Chem. Rev.*, 1995, **95**, 69–96.

123 J. Peral, X. Domènech and D. F. Ollis, *J. Chem. Technol. Biotechnol.*, 1997, **70**, 117–140.

124 J. Saien and A. R. Soleymani, *J. Ind. Eng. Chem.*, 2012, **18**, 1683–1688.

125 J. Zhao, C. Chen and W. Ma, *Top. Catal.*, 2005, **35**, 269–278.

126 C. Galindo, P. Jacques and A. Kalt, *J. Photochem. Photobiol., A*, 2000, **130**, 35–47.

127 Y. Ma and J.-n. Yao, *J. Photochem. Photobiol., A*, 1998, **116**, 167–170.

128 F. Chen, Y. Xie, J. Zhao and G. Lu, *Chemosphere*, 2001, **44**, 1159–1168.

129 F. Zhang, J. Zhao, T. Shen, H. Hidaka, E. Pelizzetti and N. Serpone, *Appl. Catal., B*, 1998, **15**, 147–156.

130 H. Zhu, R. Jiang, Y. Fu, Y. Guan, J. Yao, L. Xiao and G. Zeng, *Desalination*, 2012, **286**, 41–48.

131 M. Behnajady, N. Modirshahla and R. Hamzavi, *J. Hazard. Mater.*, 2006, **133**, 226–232.

132 S. K. Kansal, M. Singh and D. Sud, *J. Hazard. Mater.*, 2008, **153**, 412–417.

133 M. Muruganandham and M. Swaminathan, *Sol. Energy Mater. Sol. Cells*, 2004, **81**, 439–457.

134 S. Sakthivel, B. Neppolian, M. Shankar, B. Arabindoo, M. Palanichamy and V. Murugesan, *Sol. Energy Mater. Sol. Cells*, 2003, **77**, 65–82.

135 M. Qamar, M. Saquib and M. Muneer, *Dyes Pigm.*, 2005, **65**, 1–9.

136 S. Tunesi and M. Anderson, *J. Phys. Chem.*, 1991, **95**, 3399–3405.

137 M. S. Goncalves, A. M. Oliveira-Campos, E. M. Pinto, P. Plasência and M. J. R. Queiroz, *Chemosphere*, 1999, **39**, 781–786.

138 A. H. Mahvi, M. Ghanbarian, S. Nasseri and A. Khairi, *Desalination*, 2009, **239**, 309–316.

139 W. Baran, A. Makowski and W. Wardas, *Chemosphere*, 2003, **53**, 87–95.

140 W. Z. Tang and R. Z. Chen, *Chemosphere*, 1996, **32**, 947–958.

141 B. Neppolian, H. Choi, S. Sakthivel, B. Arabindoo and V. Murugesan, *Chemosphere*, 2002, **46**, 1173–1181.

142 E. Bizani, K. Fytianos, I. Poulios and V. Tsiridis, *J. Hazard. Mater.*, 2006, **136**, 85–94.

143 J. Wiszniewski, D. Robert, J. Surmacz-Gorska, K. Miksch and J.-V. Weber, *J. Photochem. Photobiol. A*, 2002, **152**, 267–273.

144 C. Raillard, V. Héquet, P. Le Cloirec and J. Legrand, *Water Sci. Technol.*, 2004, **50**, 241–250.

145 D. Hufschmidt, D. Bahnemann, J. J. Testa, C. A. Emilio and M. I. Litter, *J. Photochem. Photobiol. A*, 2002, **148**, 223–231.

146 M. Vautier, *J. Catal.*, 2001, **201**, 46–59.

147 I. Poulios and I. Tsachpinis, *J. Chem. Technol. Biotechnol.*, 1999, **74**, 349–357.

148 I. Poulios, A. Avranas, E. Rekliti and A. Zouboulis, *J. Chem. Technol. Biotechnol.*, 2000, **75**, 205–212.

149 L. B. Reutergådh and M. Iangphasuk, *Chemosphere*, 1997, **35**, 585–596.

150 D. Curcó, J. Gimenez, A. Addardak, S. Cervera-March and S. Esplugas, *Catal. Today*, 2002, **76**, 177–188.

151 M. Qamar, M. Muneer and D. Bahnemann, *J. Environ. Manage.*, 2006, **80**, 99–106.

152 C. Karunakaran and S. Senthilvelan, *Catal. Commun.*, 2005, **6**, 159–165.

153 G. C. Collazzo, E. L. Foletto, S. L. Jahn and M. A. Villetti, *J. Environ. Manage.*, 2012, **98**, 107–111.

154 N. San, A. Hatipoğlu, G. Koçtürk and Z. Çınar, *J. Photochem. Photobiol. A*, 2001, **139**, 225–232.

155 C. A. Gouvea, F. Wypych, S. G. Moraes, N. Duran, N. Nagata and P. Peralta-Zamora, *Chemosphere*, 2000, **40**, 433–440.

156 M. Saquib and M. Muneer, *Dyes Pigm.*, 2002, **53**, 237–249.

157 A. F. Caliman, C. Cojocaru, A. Antoniadis and I. Poulios, *J. Hazard. Mater.*, 2007, **144**, 265–273.

158 J. Percherancier, R. Chapelon and B. Pouyet, *J. Photochem. Photobiol. A*, 1995, **87**, 261–266.

159 A. B. Prevot, M. Vincenti, B. A. and E. Pramauro, *Appl. Catal. B*, 1999, **22**, 149–158.

160 I. Poulios and I. Aetopoulou, *Environ. Technol.*, 1999, **20**, 479–487.

161 R. W. Matthews, *Sol. Energy*, 1987, **38**, 405–413.

162 M. Saquib, T. M. Abu, M. Haque and M. Muneer, *J. Environ. Manage.*, 2008, **88**, 300.

163 C. Lung-Chyuan and C. Tse-Chuan, *J. Mol. Catal.*, 1993, **85**, 201–214.

164 E. C. Ilinoiu, R. Pode, F. Manea, L. A. Colar, A. Jakab, C. Orha, C. Ratiu, C. Lazau and P. Sfarloaga, *J. Taiwan Inst. Chem. Eng.*, 2012, **44**(2), 270–278.

165 H. Wang, C. Xie, W. Zhang, S. Cai, Z. Yang and Y. Gui, *J. Hazard. Mater.*, 2007, **141**, 645–652.

166 M. N. Chong, B. Jin, C. W. Chow and C. Saint, *Water Res.*, 2010, **44**, 2997–3027.

167 C.-H. Liao, S.-F. Kang and F.-A. Wu, *Chemosphere*, 2001, **44**, 1193–1200.

168 X. Wang, J. Jia and Y. Wang, *J. Hazard. Mater.*, 2011, **185**, 315–321.

169 H. Zhu, J.-Y. Li, J.-C. Zhao and G. J. Churchman, *Appl. Clay Sci.*, 2005, **28**, 79–88.

170 A. Aguedach, S. Brosillon, J. Morvan and K. Lhadi El, *J. Hazard. Mater.*, 2008, **150**, 250–256.

171 U. Diebold, *Surf. Sci. Rep.*, 2003, **48**, 53–229.

172 X. Chen, W. Wang, H. Xiao, C. Hong, F. Zhu, Y. Yao and Z. Xue, *Chem. Eng. J.*, 2012, **193–194**, 290–295.

173 R. Venkatadri and R. W. Peters, *Hazard. Waste Hazard. Mater.*, 1993, **10**, 107–149.

174 J. Fernandez, J. Bandara, A. Lopez, P. Buffat and J. Kiwi, *Langmuir*, 1999, **15**, 185–192.

175 M. R. Dhananjeyan, E. Mielczarski, K. R. Thampi, P. Buffat, M. Bensimon, A. Kulik, J. Mielczarski and J. Kiwi, *J. Phys. Chem. B*, 2001, **105**, 12046–12055.

176 A. Bozzi, M. Dhananjeyan, I. Guasaquillo, S. Parra, C. Pulgarin, C. Weins and J. Kiwi, *J. Photochem. Photobiol. A*, 2004, **162**, 179–185.

177 S. S. Reddy and B. Kotaiah, *Int. J. Environ. Sci. Technol.*, 2005, **2**, 245–251.

178 X. Wang, Z. Yao, J. Wang, W. Guo and G. Li, *Ultrason. Sonochem.*, 2008, **15**, 43–48.

179 I. K. Kim and C. P. Huang, *J. Chin. Inst. Eng.*, 2005, **28**, 1107–1118.

180 R. Mettin, S. Luther, C.-D. Ohl and W. Lauterborn, *Ultrason. Sonochem.*, 1999, **6**, 25–29.

181 T. Leighton, *Ultrason. Sonochem.*, 1995, **2**, S123–S136.

182 S. Tangestaninejad, M. Moghadam, V. Mirkhani, I. Mohammadpoor-Baltork and H. Salavati, *Ultrason. Sonochem.*, 2008, **15**, 815–822.

183 I. Z. Shirgaonkar and A. B. Pandit, *Ultrason. Sonochem.*, 1998, **5**, 53–61.

184 N. L. Stock, J. Peller, K. Vinodgopal and P. V. Kamat, *Environ. Sci. Technol.*, 2000, **34**, 1747–1750.

185 M. Mrowetz, C. Pirola and E. Sell, *Ultrason. Sonochem.*, 2003, **10**, 247–254.

186 K. M. Kalumuck and G. L. Chahine, <http://resolver.caltech.edu/cav2001:sessionA4.006>, 2001.

187 M. Sivakumar and A. B. Pandit, *Ultrason. Sonochem.*, 2002, **9**, 123–131.

188 P. R. Gogate and A. B. Pandit, *Adv. Environ. Res.*, 2004, **8**, 501–551.

189 V. K. Saharan, A. B. Pandit, P. S. Satish Kumar and S. Anandan, *Ind. Eng. Chem. Res.*, 2011, **51**, 1981–1989.

190 Y. Deng and C. M. Ezyske, *Water Res.*, 2011, **45**, 6189–6194.

191 P. Nfodzo and H. Choi, *Chem. Eng. J.*, 2011, **174**, 629–634.

192 J. Criquet and N. K. V. Leitner, *Chemosphere*, 2009, **77**, 194–200.

193 R. H. Waldemer, P. G. Tratnyek, R. L. Johnson and J. T. Nurmi, *Environ. Sci. Technol.*, 2007, **41**, 1010–1015.

194 P. Neta, V. Madhavan, H. Zemel and R. W. Fessenden, *J. Am. Chem. Soc.*, 1977, **99**, 163–164.

195 G. P. Anipsitakis and D. D. Dionysiou, *Environ. Sci. Technol.*, 2004, **38**, 3705–3712.

196 K. B. Dhanalakshmi, S. Anandan, J. Madhavan and P. Maruthamuthu, *Sol. Energy Mater. Sol. Cells*, 2008, **92**, 457–463.

197 A. Zaleska, *Recent Pat. Eng.*, 2008, **2**, 157–164.

198 J. Zhang, Y. Wu, M. Xing, S. A. K. Leghari and S. Sajjad, *Energy Environ. Sci.*, 2010, **3**, 715–726.

199 C. Ying, D. Hao and W. Lishi, *J. Mater. Sci. Technol.*, 2008, **24**, 675–689.

200 M. Fittipaldi, V. Gombac, A. Gasparotto, C. Deiana, G. Adami, D. Barreca, T. Montini, G. Martra, D. Gatteschi and P. Fornasiero, *ChemPhysChem*, 2011, **12**, 2221–2224.

201 D. Chen, Z. Jiang, J. Geng, Q. Wang and D. Yang, *Ind. Eng. Chem. Res.*, 2007, **46**, 2741–2746.

202 Y. Zhang, H. Xu, Y. Xu, H. Zhang and Y. Wang, *J. Photochem. Photobiol. A*, 2005, **170**, 279–285.

203 W. Balcerski, S. Y. Ryu and M. R. Hoffmann, *J. Phys. Chem. C*, 2007, **111**, 15357–15362.

204 T. Tachikawa, Y. Takai, S. Tojo, M. Fujitsuka, H. Irie, K. Hashimoto and T. Majima, *J. Phys. Chem. B*, 2006, **110**, 13158–13165.

205 D. Meroni, S. Ardizzone, G. Cappelletti, C. Oliva, M. Ceotto, D. Poelman and H. Poelman, *Catal. Today*, 2011, **161**, 169–174.

206 A. Emeline, X. Zhang, M. Jin, T. Murakami and A. Fujishima, *J. Photochem. Photobiol. A*, 2009, **207**, 13–19.

207 B. Wawrzyniak and A. W. Morawski, *Appl. Catal. B*, 2006, **62**, 150–158.

208 Y. Cong, J. Zhang, F. Chen and M. Anpo, *J. Phys. Chem. C*, 2007, **111**, 6976–6982.

209 A. R. Gandhe, S. P. Naik and J. B. Fernandes, *Microporous Mesoporous Mater.*, 2005, **87**, 103–109.

210 Z. He and H. He, *Appl. Surf. Sci.*, 2011, **258**, 972–976.

211 C. Wang, M. Wang, K. Xie, Q. Wu, L. Sun, Z. Lin and C. Lin, *Nanotechnology*, 2011, **22**, 305607.

212 F. Peng, L. Cai, H. Yu, H. Wang and J. Yang, *J. Solid State Chem.*, 2008, **181**, 130–136.

213 X. Chen, Y. B. Lou, A. C. Samia, C. Burda and J. L. Gole, *Adv. Funct. Mater.*, 2005, **15**, 41–49.

214 N. Sobana and M. Swaminathan, *Sol. Energy Mater. Sol. Cells*, 2007, **91**, 727–734.

215 Y. J. Jang, C. Simer and T. Ohm, *Mater. Res. Bull.*, 2006, **41**, 67–77.

216 R. Asahi, T. Morikawa, T. Ohwaki, K. Aoki and Y. Taga, *science*, 2001, **293**, 269–271.

217 C. Di Valentin, E. Finazzi, G. Pacchioni, A. Selloni, S. Livraghi, M. C. Paganini and E. Giannello, *Chem. Phys.*, 2007, **339**, 44–56.

218 H. Irie, Y. Watanabe and K. Hashimoto, *J. Phys. Chem. B*, 2003, **107**, 5483–5486.

219 K. Parida and B. Naik, *J. Colloid Interface Sci.*, 2009, **333**, 269–276.

220 A. Selvaraj, S. Sivakumar, A. Ramasamy and V. Balasubramanian, *Res. Chem. Intermed.*, 2013, **39**, 2287–2302.

221 T. Ihara, M. Miyoshi, Y. Iriyama, O. Matsumoto and S. Sugihara, *Appl. Catal. B*, 2003, **42**, 403–409.

222 N. Serpone, *J. Phys. Chem. B*, 2006, **110**, 24287–24293.

223 P. Songkhum and J. Tantirungrotechai, *Res. Chem. Intermed.*, 2013, **39**, 1555–1561.

224 J. Sun, L. Qiao, S. Sun and G. Wang, *J. Hazard. Mater.*, 2008, **155**, 312–319.

225 B. Neumann, P. Bogdanoff, H. Tributsch, S. Sakthivel and H. Kisch, *J. Phys. Chem. B*, 2005, **109**, 16579–16586.

226 S. U. Khan, M. Al-Shahry and W. B. Ingler, *science*, 2002, **297**, 2243–2245.

227 S. Sakthivel and H. Kisch, *Angew. Chem., Int. Ed.*, 2003, **42**, 4908–4911.

228 W. Ren, Z. Aia, F. Jiaa, L. Zhang, X. Fanb and Z. Zoub, *Appl. Catal. B*, 2007, **69**, 138–144.

229 R. Velmurugan, B. Krishnakumar, B. Subash and M. Swaminathan, *Sol. Energy Mater. Sol. Cells*, 2013, **108**, 205–212.

230 K. Ranjit, I. Willner, S. Bossmann and A. Braun, *Environ. Sci. Technol.*, 2001, **35**, 1544–1549.

231 A.-W. Xu, Y. Gao and H.-Q. Liu, *J. Catal.*, 2002, **207**, 151–157.

232 D. W. Hwang, J. S. Lee, W. Li and S. H. Oh, *J. Phys. Chem. B*, 2003, **107**, 4963–4970.

233 S. Matsuo, N. Sakaguchi, K. Yamada, T. Matsuo and H. Wakita, *Appl. Surf. Sci.*, 2004, **228**, 233–244.

234 Y. Wang, H. Cheng, L. Zhang, Y. Hao, J. Ma, B. Xu and W. Li, *J. Mol. Catal. A: Chem.*, 2000, **151**, 205–216.

235 Y. Zhang, H. Zhang, Y. Xu and Y. Wang, *J. Solid State Chem.*, 2004, **177**, 3490–3498.

236 X. Zhang, M. Zhou and L. Lei, *Carbon*, 2005, **43**, 1700–1708.

237 Y. Xie, C. Yuan and X. Li, *Colloids Surf. A*, 2005, **252**, 87–94.

238 Y. Xie, C. Yuan and X. Li, *Mater. Sci. Eng., B*, 2005, **117**, 325–333.

239 W. Zhang, X. Li, G. Jia, Y. Gao, H. Wang, Z. Cao, C. Li and J. Liu, *Catal. Commun.*, 2014, **45**, 144–147.

240 X. Lan, L. Wang, B. Zhang, B. Tian and J. Zhang, *Catal. Today*, 2014, **224**, 163–170.

241 M. Nasir, J. Zhang, F. Chen and B. Tian, *Res. Chem. Intermed.*, 2013, 1–18.

242 M. Nasir, Z. Xi, M. Xing, J. Zhang, F. Chen, B. Tian and S. Bagwasi, *J. Phys. Chem. C*, 2013, **117**, 9520–9528.

243 T. Yu, X. Tan, L. Zhao, Y. Yin, P. Chen and J. Wei, *Chem. Eng. J.*, 2010, **157**, 86–92.

244 W. Choi, A. Termin and M. R. Hoffmann, *J. Phys. Chem.*, 1994, **98**, 13669–13679.

245 L. Andronic, A. Enesca, C. Vladuta and A. Duta, *Chem. Eng. J.*, 2009, **152**, 64–71.

246 X. S. Li, G. E. Fryxell, M. H. Engelhard and C. Wang, *Inorg. Chem. Commun.*, 2007, **10**, 639–641.

247 H. Chun, T. Yuchao and T. Hongxiao, *Catal. Today*, 2004, **90**, 325–330.

248 M. Di Paola, P. Zaccagnino, G. Montedoro, T. Cocco and M. Lorusso, *J. Bioenerg. Biomembr.*, 2004, **36**, 165–170.

249 I. H. Tseng, J. C. S. Wu and H.-Y. Chou, *J. Catal.*, 2004, **221**, 432–440.

250 F. Zhuge, X. Li, X. Gao, X. Gan and F. Zhou, *Mater. Lett.*, 2009, **63**, 652–654.

251 A. A. Sagade and R. Sharma, *Sens. Actuators, B*, 2008, **133**, 135–143.

252 L. Andronic, L. Isac and A. Duta, *J. Photochem. Photobiol. A*, 2011, **221**, 30–37.

253 L. Huang, F. Peng, H. Yu and H. Wang, *Solid State Sci.*, 2009, **11**, 129–138.

254 F. Sayilan, M. Asilturk, P. Tatar, N. Kiraz, E. Arpac and H. Sayilan, *J. Hazard. Mater.*, 2007, **144**, 140–146.

255 M. K. Seery, R. George, P. Floris and S. C. Pillai, *J. Photochem. Photobiol. A*, 2007, **189**, 258–263.

256 M. V. Liga, E. L. Bryant, V. L. Colvin and Q. Li, *Water Res.*, 2011, **45**, 535–544.

257 C. Sun, Q. Li, S. Gao, L. Cao and J. K. Shang, *J. Am. Ceram. Soc.*, 2010, **93**, 3880–3885.

258 P. Wu, R. Xie, K. Imlay and J. K. Shang, *Environ. Sci. Technol.*, 2010, **44**, 6992–6997.

259 A. L. Linsebigler, G. Lu and J. T. Yates Jr, *Chem. Rev.*, 1995, **95**, 735–758.

260 D. Behar and J. Rabani, *J. Phys. Chem. B*, 2006, **110**, 8750–8755.

261 X. You, F. Chen, J. Zhang and M. Anpo, *Catal. Lett.*, 2005, **102**, 247–250.

262 A. Gupta, A. Pal and C. Sahoo, *Dyes Pigm.*, 2006, **69**, 224–232.

263 C. Gunawan, W. Y. Teoh, C. P. Marquis, J. Lifia and R. Amal, *Small*, 2009, **5**, 341–344.

264 S. T. Hussain, Rashid, D. Anjum, A. Siddiqua and A. Badshah, *Mater. Res. Bull.*, 2013, **48**, 705–714.

265 S. Sato, J. M. White and T. U. A. A. D. O. CHEMISTRY, *Photodecomposition of Water Over Pt/TiO<sub>2</sub> Catalysts*, Defense Technical Information Center, 1980.

266 S. Sato and J. White, *J. Phys. Chem.*, 1981, **85**, 592–594.

267 I. Izumi, F.-R. F. Fan and A. J. Bard, *J. Phys. Chem.*, 1981, **85**, 218–223.

268 M. S. John, A. Furgala and A. Sammells, *J. Electrochem. Soc.*, 1982, **129**, 246–250.

269 H. Einaga, M. Harada, S. Futamura and T. Ibusuki, *J. Phys. Chem. B*, 2003, **107**, 9290–9297.

270 Y. Gai, J. Li, S.-S. Li, J.-B. Xia and S.-H. Wei, *Phys. Rev. Lett.*, 2009, **102**, 036402.

271 T. Ohno, Z. Miyamoto, K. Nishijima, H. Kanemitsu and F. Xueyuan, *Appl. Catal. A*, 2006, **302**, 62–68.

272 M. Y. Xing, D. Y. Qi, J. L. Zhang and F. Chen, *Chem.-Eur. J.*, 2011, **17**, 11432–11436.

273 F. Yang, H. Yang, B. Tian, J. Zhang and D. He, *Res. Chem. Intermed.*, 2013, **39**, 1685–1699.

274 L. Yan, Y. Cheng, S. Yuan, X. Yan, X. Hu and K. Oh, *Res. Chem. Intermed.*, 2013, **39**, 1673–1684.

275 U. G. Akpan and B. H. Hameed, *Chem. Eng. J.*, 2011, **169**, 91–99.

276 M. Zhang, C. Chen, W. Ma and J. Zhao, *Angew. Chem.*, 2008, **120**, 9876–9879.

277 H. Zhang, R. Zong, J. Zhao and Y. Zhu, *Environ. Sci. Technol.*, 2008, **42**, 3803–3807.

278 H.-c. Liang and X.-z. Li, *Appl. Catal. B*, 2009, **86**, 8–17.

279 A. E. Regazzoni, P. Mandelbaum, M. Matsuyoshi, S. Schiller, S. A. Bilmes and M. A. Blesa, *Langmuir*, 1998, **14**, 868–874.

280 J. Moser, S. Punchihewa, P. P. Infelta and M. Graetzel, *Langmuir*, 1991, **7**, 3012–3018.

281 S. Ikeda, C. Abe, T. Torimoto and B. Ohtani, *J. Photochem. Photobiol. A*, 2003, **160**, 61–67.

282 B. Zhang, W. Zou and J. Zhang, *Res. Chem. Intermed.*, 2010, 1–14.

283 A. Di Paola, E. Garcia-Lopez, G. Marci and L. Palmisano, *J. Hazard. Mater.*, 2012, **211–212**, 3–29.

284 G. K. Mor, O. K. Varghese, M. Paulose, K. Shankar and C. A. Grimes, *Sol. Energy Mater. Sol. Cells*, 2006, **90**, 2011–2075.

285 H.-F. Zhuang, C.-J. Lin, Y.-K. Lai, L. Sun and J. Li, *Environ. Sci. Technol.*, 2007, **41**, 4735–4740.

286 L. K. Tan, M. K. Kumar, W. W. An and H. Gao, *ACS Appl. Mater. Interfaces*, 2010, **2**, 498–503.

287 J. Toledo Antonio, M. Cortes-Jacome, S. Orozco-Cerros, E. Montiel-Palacios, R. Suarez-Parra, C. Angeles-Chavez, J. Navarete and E. López-Salinas, *Appl. Catal. B*, 2010, **100**, 47–54.

288 H. Xu, G. Vanamu, Z. Nie, H. Konishi, R. Yeredla, J. Phillips and Y. Wang, *J. Nanomater.*, 2006, **2006**, 23.

289 J. M. Macak, M. Zlamal, J. Krysa and P. Schmuki, *Small*, 2007, **3**, 300–304.

290 Y. Lai, L. Sun, Y. Chen, H. Zhuang, C. Lin and J. W. Chin, *J. Electrochem. Soc.*, 2006, **153**, D123–D127.

291 Y. Wang, R. Shi, J. Lin and Y. Zhu, *Appl. Catal. B*, 2010, **100**, 179–183.

292 M. Ishigami, J. Chen, W. Cullen, M. Fuhrer and E. Williams, *Nano Lett.*, 2007, **7**, 1643–1648.

293 H. Zhang, X. Lv, Y. Li, Y. Wang and J. Li, *ACS Nano*, 2009, **4**, 380–386.

294 B. Qiu, M. Xing and J. Zhang, *J. Am. Chem. Soc.*, 2014, **136**, 5852–5855.

295 V. Krishna, N. Noguchi, B. Koopman and B. Moudgil, *J. Colloid Interface Sci.*, 2006, **304**, 166–171.

296 W.-C. Oh, A.-R. Jung and W.-B. Ko, *J. Ind. Eng. Chem.*, 2007, **13**, 1208–1214.

297 S. Mu, Y. Long, S.-Z. Kang and J. Mu, *Catal. Commun.*, 2010, **11**, 741–744.

298 H. G. Yang, G. Liu, S. Z. Qiao, C. H. Sun, Y. G. Jin, S. C. Smith, J. Zou, H. M. Cheng and G. Q. Lu, *J. Am. Chem. Soc.*, 2009, **131**, 4078–4083.

299 J. S. Chen, Y. L. Tan, C. M. Li, Y. L. Cheah, D. Luan, S. Madhavi, F. Y. C. Boey, L. A. Archer and X. W. Lou, *J. Am. Chem. Soc.*, 2010, **132**, 6124–6130.

300 S. Liu, J. Yu and M. Jaroniec, *J. Am. Chem. Soc.*, 2010, **132**, 11914–11916.

301 H. Yu, B. Tian and J. Zhang, *Chem.-Eur. J.*, 2011, **17**, 5499–5502.

302 I. M. Arabatzis, S. Antonaraki, T. Stergiopoulos, A. Hiskia, E. Papaconstantinou, M. C. Bernard and P. Falaras, *J. Photochem. Photobiol. A*, 2002, **149**, 237–245.

303 K. Kabra, R. Chaudhary and R. L. Sawhney, *Ind. Eng. Chem. Res.*, 2004, **43**, 7683–7696.

304 N. Bao, X. Feng, Z. Yang, L. Shen and X. Lu, *Environ. Sci. Technol.*, 2004, **38**, 2729–2736.

305 V. Loddo, G. Marci, L. Palmisano and A. Sclafani, *Mater. Chem. Phys.*, 1998, **53**, 217–224.

306 Y. G. Adewuyi, *Environ. Sci. Technol.*, 2005, **39**, 8557–8570.

307 A. Masarwa, S. Rachmilovich-Calis, N. Meyerstein and D. Meyerstein, *Coord. Chem. Rev.*, 2005, **249**, 1937–1943.

308 E. Chamarro, A. Marco and S. Esplugas, *Water Res.*, 2001, **35**, 1047–1051.

309 B. Mounir, M.-N. Pons, O. Zahraa, A. Yaacoubi and A. Benhammou, *J. Hazard. Mater.*, 2007, **148**, 513–520.

310 S. Fukahori, H. Ichiura, T. Kitaoka and H. Tanaka, *Environ. Sci. Technol.*, 2003, **37**, 1048–1051.

311 M. Karches, M. Morstein, P. Rudolf von Rohr, R. L. Pozzo, J. L. Giombi and M. A. Baltanás, *Catal. Today*, 2002, **72**, 267–279.

312 T.-H. Kim, C. Park and S. Kim, *J. Cleaner Prod.*, 2005, **13**, 779–786.

313 M. A. Behnajady, N. Modirshahla, M. Shokri, H. Elham and A. Zeininezhad, *J. Environ. Sci. Health, Part A: Toxic/Hazard. Subst. Environ. Eng.*, 2008, **43**, 460–467.

314 Y. M. Xu, P. E. Ménassa and C. H. Langford, *Chemosphere*, 1988, **17**, 1971–1976.

315 A. Y. Shan, T. I. M. Ghazi and S. A. Rashid, *Appl. Catal., A*, 2010, **389**, 1–8.

316 C.-H. Huang, K.-P. Chang, H.-D. Ou, Y.-C. Chiang, E.-E. Chang and C.-F. Wang, *J. Hazard. Mater.*, 2011, **186**, 1174–1182.

317 C.-C. Wang, C.-K. Lee, M.-D. Lyu and L.-C. Juang, *Dyes Pigm.*, 2008, **76**, 817–824.

318 M. Nikazar, K. Gholivand and K. Mahanpoor, *Desalination*, 2008, **219**, 293–300.

319 H. Zhu, R. Jiang, L. Xiao, Y. Chang, Y. Guan, X. Li and G. Zeng, *J. Hazard. Mater.*, 2009, **169**, 933–940.

320 L. Rizzo, J. Koch, V. Belgiorno and M. A. Anderson, *Desalination*, 2007, **211**, 1–9.

321 H. Zhang and L. Yang, *Thin Solid Films*, 2012, **520**, 5922–5927.

322 M. A. Behnajady, N. Modirshahla, N. Daneshvar and M. Rabbani, *Chem. Eng. J.*, 2007, **127**, 167–176.

323 R. W. Matthews, *Water Res.*, 1991, **25**, 1169–1176.

324 O. Carp, C. L. Huisman and A. Reller, *Prog. Solid State Chem.*, 2004, **32**, 33–177.

325 R. W. Matthews, *J. Catal.*, 1988, **111**, 264–272.

326 Y. Kuwahara, T. Kamegawa, K. Mori and H. Yamashita, *Chem. Commun.*, 2008, **2008**, 4783–4785.

327 N. O. Gopal, H.-H. Lo and S.-C. Ke, *J. Am. Chem. Soc.*, 2008, **130**, 2760–2761.

328 M. Xing, D. Qi, J. Zhang, F. Chen, B. Tian, S. Bagwas and M. Anpo, *J. Catal.*, 2012, **294**, 37–46.

329 M. Xing, W. Fang, M. Nasir, Y. Ma, J. Zhang and M. Anpo, *J. Catal.*, 2013, **297**, 236–243.

330 D. Qi, M. Xing and J. Zhang, *J. Phys. Chem. C*, 2014, **118**, 7329–7336.

331 G. A. Roberts, *Chitin chemistry*, Macmillan, 1992.

332 M. N. Ravi Kumar, *React. Funct. Polym.*, 2000, **46**, 1–27.

333 I. Aranaz, M. Mengíbar, R. Harris, I. Paños, B. Miralles, N. Acosta, G. Galed and Á. Heras, *Curr. Chem. Biol.*, 2009, **3**, 203–230.

334 W. Ngah and S. Fatinathan, *Chem. Eng. J.*, 2008, **143**, 62–72.

335 D. Chauhan and N. Sankararamakrishnan, *Bioresour. Technol.*, 2008, **99**, 9021–9024.

336 A.-H. Chen, S.-C. Liu, C.-Y. Chen and C.-Y. Chen, *J. Hazard. Mater.*, 2008, **154**, 184–191.

337 C. E. Zubieta, P. V. Messina, C. Luengo, M. Dennehy, O. Pieroni and P. C. Schulz, *J. Hazard. Mater.*, 2008, **152**, 765–777.

338 Z. Zainal, L. K. Hui, M. Z. Hussein, A. H. Abdullah and I. R. Hamadneh, *J. Hazard. Mater.*, 2009, **164**, 138–145.

339 R. Jiang, H. Zhu, X. Li and L. Xiao, *Chem. Eng. J.*, 2009, **152**, 537–542.

340 X. Wang, Y. Du, S. Ding, L. Fan, X. Shi, Q. Wang and G. Xiong, *Phys. E*, 2005, **30**, 96–100.

341 R. Khan, A. Kaushik, P. R. Solanki, A. A. Ansari, M. K. Pandey and B. Malhotra, *Anal. Chim. Acta*, 2008, **616**, 207–213.

342 J.-Y. Chen, P.-J. Zhou, J.-L. Li and Y. Wang, *Carbohydr. Polym.*, 2008, **72**, 128–132.

343 P. Serp, M. Corrias and P. Kalck, *Appl. Catal., A*, 2003, **253**, 337–358.

344 M. M. Nassar and M. S. El-Geundi, *J. Chem. Technol. Biotechnol.*, 1991, **50**, 257–264.

345 F. Rodriguez-Reinoso, *Carbon*, 1998, **36**, 159–175.

346 G. Li Puma, A. Bono, D. Krishnaiah and J. G. Collin, *J. Hazard. Mater.*, 2008, **157**, 209–219.

347 B. Tryba, *Int. J. Photoenergy*, 2008, 2008.

348 J. Matos, J. Laine and J.-M. Herrmann, *J. Catal.*, 2001, **200**, 10–20.

349 S. X. Liu, X. Y. Chen and X. Chen, *J. Hazard. Mater.*, 2007, **143**, 257–263.

350 Y. Ao, J. Xu, S. Zhang and D. Fu, *Appl. Surf. Sci.*, 2010, **256**, 2754–2758.

351 T. Cordero, J.-M. Chovelon, C. Duchamp, C. Ferronato and J. Matos, *Appl. Catal., B*, 2007, **73**, 227–235.

352 C. Raghavacharya, *Chem. Eng. World*, 1997, **32**, 53–54.

353 J. Araña, J. Dona-Rodríguez, E. Tello Rendón, C. Garriga i Cabo, O. González-Díaz, J. Herrera-Melián, J. Pérez-Peña, G. Colón and J. Navío, *Appl. Catal., B*, 2003, **44**, 153–160.

354 X. Zhang, M. Zhou and L. Lei, *Carbon*, 2006, **44**, 325–333.

355 D.-K. Lee, S.-C. Kim, S.-J. Kim, I.-S. Chung and S.-W. Kim, *Chem. Eng. J.*, 2004, **102**, 93–98.

356 X. Ma, S. Wang, J. Gong, X. Yang and G. Xu, *J. Mol. Catal. A: Chem.*, 2004, **222**, 183–187.

357 A. Fernandez, G. Lassaletta, V. Jimenez, A. Justo, A. Gonzalez-Elipe, J.-M. Herrmann, H. Tahiri and Y. Ait-Ichou, *Appl. Catal., B*, 1995, **7**, 49–63.

358 P. Yuan, D. Wu, H. He and Z. Lin, *Appl. Surf. Sci.*, 2004, **227**, 30–39.

359 G. Tian, H. Fu, L. Jing, B. Xin and K. Pan, *J. Phys. Chem. C*, 2008, **112**, 3083–3089.

360 J. Xu, Y. Ao, D. Fu and C. Yuan, *J. Phys. Chem. Solids*, 2008, **69**, 2366–2370.

361 Z. Sun, C. Bai, S. Zheng, X. Yang and R. L. Frost, *Appl. Catal., A*, 2013, **458**, 103–110.

362 D. Eder, *Chem. Rev.*, 2010, **110**, 1348–1385.

363 Y. Yu, J. C. Yu, J.-G. Yu, Y.-C. Kwok, Y.-K. Che, J.-C. Zhao, L. Ding, W.-K. Ge and P.-K. Wong, *Appl. Catal., A*, 2005, **289**, 186–196.

364 Q. Wang, D. Yang, D. Chen, Y. Wang and Z. Jiang, *J. Nanopart. Res.*, 2007, **9**, 1087–1096.

365 W. Oh and M. Chen, *Bull. Korean Chem. Soc.*, 2008, **29**, 159.

366 H. Yu, X. Quan, S. Chen, H. Zhao and Y. Zhang, *J. Photochem. Photobiol., A*, 2008, **200**, 301–306.

367 Y. Yao, G. Li, S. Ciston, R. M. Lueptow and K. A. Gray, *Environ. Sci. Technol.*, 2008, **42**, 4952–4957.

368 Y. Yu, J. C. Yu, C.-Y. Chan, Y.-K. Che, J.-C. Zhao, L. Ding, W.-K. Ge and P.-K. Wong, *Appl. Catal., B*, 2005, **61**, 1–11.

369 Y. Luo, J. Liu, X. Xia, X. Li, T. Fang, S. Li, Q. Ren, J. Li and Z. Jia, *Mater. Lett.*, 2007, **61**, 2467–2472.

370 D. Chowdhury, A. Paul and A. Chattopadhyay, *Langmuir*, 2005, **21**, 4123–4128.

371 Y. Cheng, L. An, F. Gao, G. Wang, X. Li and X. Chen, *Res. Chem. Intermed.*, 2013, **39**, 3969–3979.